



Global Snow Monitoring for Climate Research

Algorithm Theoretical Basis Document – SE-algorithm

EUROPEAN SPACE AGENCY STUDY CONTRACT REPORT
ESRIN Contract 21703/08/I-EC

DELIVERABLE 09

PREPARED BY

SARI METSÄMÄKI, MIIA SALMINEN (SYKE); JOUNI PULLIAINEN, KARI LUOJUS (FMI); THOMAS NAGLER, GABRIELE BIPPUS (ENVEO); RUNE SOLBERG, ARNT-BØRRE SALBERG, ØIVIND DUE TRIER (NR); ANDREAS WIESMANN (GAMMA)

GLOBsnow CONSORTIUM

FINNISH METEOROLOGICAL INSTITUTE (FMI) - PRIME CONTRACTOR

ENVEO IT GMBH (ENVEO)

ENVIRONMENT CANADA (EC)

FINNISH ENVIRONMENT INSTITUTE (SYKE)

GAMMA REMOTE SENSING RESEARCH AND CONSULTING AG (GAMMA)

NORTHERN RESEARCH INSTITUTE (NORUT)

NORWEGIAN COMPUTING CENTER (NR)

METEOSWISS

UNIVERSITY OF BERN (UNIBE)

CENTRAL INSTITUTE FOR METEOROLOGY AND GEODYNAMICS (ZAMG)

ESA TECHNICAL OFFICER: SIMON PINNOCK

DATE: 28 October 2014

VERSION / REVISION: 1.3 / 02



UNIVERSITÄT
BERN



This page is intentionally left blank.

DOCUMENT CHANGE LOG

Issue/ Revision	Date	Authors	Checked by	Observations
1.0/01	12 Feb 2013	Sari Metsämäki		Initialization of the document, Section 2.4
1.0/02	21 Feb 2013	Sari Metsämäki		Section 2.3.1
1.0/03	26 Feb 2013	Sari Metsämäki, Jouni Pulliainen, Miia Salminen		All Sections
1.0/04	28 Feb 2013	Sari Metsämäki, Miia Salminen, Jouni Pulliainen, Rune Solberg		All Sections, editing
1.0/05	01 March 2013	Sari Metsämäki, Miia Salminen, Rune Solberg Andreas Wiesmann Gabriele Bippus	Sari Metsämäki	All Sections, editing
1.1/01	09 April 2013	Sari Metsämäki	Sari Metsämäki	Section 2.1 description of products All sections checking spelling errors
1.2/01	08 May 2013	Sari Metsämäki Rune Solberg Arnt-Borre Salberg Øivind Due Trier	Sari Metsämäki	Section 2.6.1.small updates Section 2.6.2, 2.7.3 and 2.7.4 added

1.2/02	6 Nov 2013	Miia Salminen	Miia Salminen	Sections 2.6, 2.7, 3, 4
1.2/03	17 Feb 2014	Miia Salminen	Jouni Pulliainen	Sections 2.6, 2.7, 3
1.3/01	27 March 2014	Sari Metsämäki	Sari Metsämäki	Sections 2.5.-2.7,
1.3/02	28 October 2014	Sari Metsämäki		all sections in general general revision (figure numbering, typos)

This page is intentionally left blank.

Table of Contents

1	Introduction	7
1.1	Purpose of the Document	7
1.2	Structure of the Document	7
1.3	Acronyms	7
1.4	Applicable Documents	8
2	Snow Extent algorithm	9
2.1	Introduction	9
2.2	Product format.....	11
2.3	Pre-Processing.....	11
2.4	Cloud Detection	13
2.5	Fractional Snow Cover Retrieval Algorithm	15
2.5.1	Hemispheric transmissivity generation	17
2.6	Snow-free ground reflectance map	20
2.6.1	Snow-free ground reflectance map for plains	20
2.6.2	Snow-free ground reflectance map for mountains	26
2.6.3	Consideration of snow-free ground reflectance in the GlobSnow SE product .	36
2.7	Estimation of uncertainties.....	37
2.7.1	Introduction.....	37
2.7.2	Uncertainties for plains	38
2.7.3	Uncertainties for mountains.....	41
2.7.4	Combining of uncertainty models	48
2.8	Time-Series Aggregation	49
2.9	Post-Processing	49
2.10	Generation of Auxiliary Data.....	50
3	SUMMARY.....	53
4	References	55

This page is intentionally left blank.

1 INTRODUCTION

1.1 Purpose of the Document

The main purpose of this document is to give a detailed description of the algorithms for generating the GlobSnow Snow Extent (SE) product v2.0 and v2.1 – featuring Fractional Snow Cover (FSC) at pixel level - used for Essential Climate Variable (ECV) on Snow Extent. SE v2.1 provides an improvement to v2.0 in terms of geolocation as the the AATSR-based products; the algorithms, auxiliary datasets etc. are the same so the descriptions given in this document are valid for both v2.0 and v2.1.

1.2 Structure of the Document

Section 2 provides a description of the algorithm for Snow Extent generation. The main modules are described in detail, including pre-processing, cloud detection, fractional snow cover retrieval, uncertainty estimation and time series aggregation. The principles of the method for Fractional Snow Cover (FSC) are described in Section 2.5. The generation of auxiliary data required as input for SE algorithm is also presented.

1.3 Acronyms

AATSR	Advanced Along-Track Scanning Radiometer (instrument of Envisat)
ATSR-2	Along-Track Scanning Radiometer 2 (instrument of ERS-2)
BEAM	Basic ERS and Envisat (A)ATSR and MERIS Toolbox
DEM	Digital Elevation Model
ENVEO	Environmental Earth Observation IT GmbH
ENVISAT	Environmental Satellite of ESA
EO	Earth Observation
ERS	European Remote Sensing satellite of ESA
ESA	European Space Agency
FCDR	Fundamental Climate Data Record
FMI	Finnish Meteorological Institute
FPS	Full Product Set
FSC	Fractional Snow Cover
MODIS	Moderate Resolution Imaging Spectro-radiometer (instrument of Terra)
MERIS	Medium Resolution Imaging Spectrometer (instrument of Envisat)
NDSI	Normalized Difference Snow Index
NR	Norwegian Computing Center
NRT	Near Real Time
PDF	Probability Density Function
RMS	Root Mean Square
RMSE	Root Mean Square Error
SCA	Snow Covered Area
SCDA	Simple Cloud Detection Algorithm
SD	Snow Depth
SE	Snow Extent
SoW	Statement of Work

SWE	Snow Water Equivalent
SYKE	Finnish Environment Institute
TOA	Top of Atmosphere
TS	Technical Specification

1.4 Applicable Documents

- [RD-1] EOEP-DUEP-EOPS-SW-08-0006. Statement of Work - DUE GlobSnow.
- [RD-2] GlobSnow Proposal - Technical Annex. Proposed by FMI et al., 2008.
- [D 1.4] Requirement Baseline Document (RB), GlobSnow team, 2009.
- [D 1.5] Ground Data Documentation (GDD), GlobSnow team, 2009.
- [D 1.6] Description of the Diagnostic Data Set (DDS), GlobSnow team, 2009.
- [D 1.7] Design Justification File, Version 1 (DJF), GlobSnow team, 2009.
- [D 1.8] Technical Specifications (TS), GlobSnow team, 2009.
- [D 1.9] Design Justification File, Version 2 (DJF), GlobSnow team, 2009.
- [D 1.10] Acceptance and Test Document (ATD), GlobSnow team, 2009.
- [D 1.11] Design Definition File (DDF), GlobSnow team, 2009.
- [D 1.12] Qualification Review Report (QRR), GlobSnow team, 2009.
- [D 1.13] Prototype Validation and Assessment Report (PVAR), GlobSnow team, 2009.
- [D 2.3] Acceptance Review Report (ARR), GlobSnow team, 2010.
- [D 2.5] Design Justification File 3 (DJF-v3), GlobSnow team 2011
- [D 2.6] Production and Validation Report (PVR), GlobSnow team, 2011.
- [D 3.1] Service Evolution Report (SER) v1, GlobSnow team, 2011.
- [D 3.2] Service Evolution Report (SER-v2) v2, GlobSnow team, 2011.
- [D 3.5] Final Report (FR), GlobSnow team, 2011.
- [RD-3] Statement of Work for GlobSnow-2 EOEP-STRI-EOPS-SW-11-0003, issue 1 revision 0.
- [RD-4] GlobSnow-2 Consolidated Proposal. Proposed by FMI et al., 2012.

2 SNOW EXTENT ALGORITHM

2.1 Introduction

The Daily Fractional Snow Cover (DFSC) product provides fractional snow cover (FSC) in percentage (%) per grid cell for all satellite overpasses of a given day. The product represents the best estimate of today's snow cover, given the sensor capabilities (ATSR-2 or AATSR). If there are multiple snow observations (only far north within a day), the satellite observations applied are those giving best solar illumination (highest solar elevation). The FSC is provided only for observations at sun zenith angle $< 73^\circ$.

The Daily 4-classes Snow Cover (D4SC) product provides snow cover classified into four categories per grid cell for all satellite overpasses of a given day. In terms of FSC, the four classes represent:

- $0\% \leq \text{FSC} \leq 10\%$
- $10\% < \text{FSC} \leq 50\%$
- $50\% < \text{FSC} \leq 90\%$
- $90\% < \text{FSC} \leq 100\%$

The Weekly Aggregated Fractional Snow Cover (WFSC) product is based on all satellite overpasses within a seven-day period. The product represents the best estimate of the current snow cover. It is generated daily, based on DFSC products within a sliding past 7-days' time window.

The Monthly Aggregated Fractional Snow Cover (MFSC) product is based on all satellite overpasses within a calendar month period. The product provides statistics for cloud-free observations of FSC within the period. It is based on DFSC products for the given calendar month.

A high-level conceptual diagram of the SE processing system is given in Figure 2.1.1

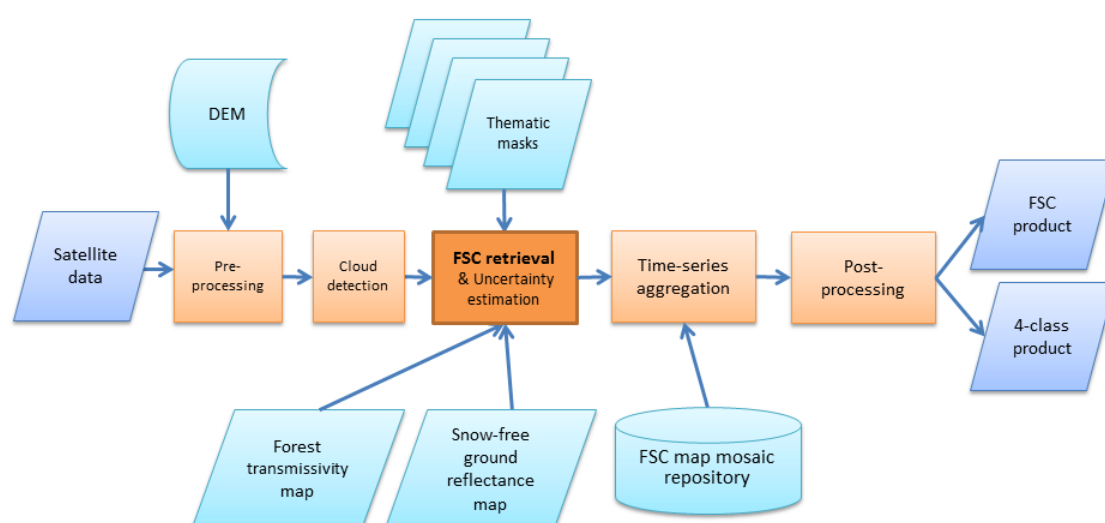


Figure 2.1.1 Conceptual model for the SE processing system.

The main data elements and buildings blocks of the system are:

1. Satellite data: ATSR-2 and AATSR data as processed and delivered from the ESA
2. Pre-processing: Geometrical correction (geo-referencing), radiometrical correction (topographic correction) and
3. Cloud detection
4. DEM: Digital Elevation Model data applied for topographic geometrical and radiometrical correction
5. FSC retrieval algorithm and uncertainty estimation
6. Thematic masks: Providing thematic map information, like forest, mountain, water etc.
7. Forest transmissivity map: applied in the FSC retrieval algorithm
8. Snow-free ground reflectance map
9. Time-series aggregation: Algorithm aggregating satellite data over a period (a few days) in order to obtain better spatial coverage
10. Post-processing: Product generation from the FSC map and uncertainty data coming from the retrieval algorithms
11. FSC and 4-classes products: Final SE products, including data on accuracy and other metadata.

The processing system will be tailored to ERS-2 ATSR-2 and Envisat AATSR data. But, the system will also be suited for processing data from other optical satellites, including MODIS and Sentinel-3 OLCI and SLSTR data to be launched in the near future.

The geo-referencing is to transfer the data from an image coordinate system (determined by how the sensor works and the acquisition geometry and timing in general) to a well-defined map system. Geometrical topographic effects have to be compensated for as well. The radiometric topographic correction is to transfer the data into standard illumination geometry, also compensating for topographic effects.

The cloud detection algorithm was particularly developed for GlobSnow purposes and is designed to discriminate clouds and snow and to avoid false cloud commissions over snow-line with thin or fractional snow cover.

The algorithm for Fractional Snow Cover (FSC) retrieval is SCAMod-method developed at SYKE.

The transmissivity map is essential to the SCAMod algorithm, describing the transparency of forest canopy which is then accounted for in the FSC-estimation.

The thematic masks assist in masking out areas not to be processed (like open water and glacier) and are also used in generation of auxiliary data for SE-processing (reflectance climatology) as well in the uncertainty calculations.

In order to increase the spatial coverage, satellite observations are aggregated over a few days. The aggregation mosaics the snow maps resulting from various satellite passes into a consolidated map.

The main tasks for the post-processing system are to classify the FSC product into the 4-classes snow product and to generate/format metadata. Metadata includes data on the accuracy of the product based on auxiliary algorithm output and reliability models for the retrieval algorithms.

2.2 Product format

The overall characteristic of the SE product is specified in Table 2.1.

Table 2.1 Overall characteristics of the SE product.

<i>Subject</i>	<i>Specifications/Comments</i>
Variable	Fractional Snow Cover (FSC) and snow cover in a 4-classes scheme
Units of variable	Percentage for FSC and categorical labels for 4-classes scheme
Coverage	Global (omitting areas where snow never occurs and areas periodically affected by the polar night)
Time period	Starting 1995
Temporal frequency	Daily Products (Level 2A) and Aggregated Products (Level 3)
Coordinate system	Lat/lon, WGS 84
Spatial resolution	0.01 × 0.01 degrees
Geometrical accuracy	Sub-pixel (aiming at 0.5 pixel)
Thematic accuracy	Aiming at 5% (maximum error of omission and commission of snow area)
Data format	GEOTIFF and NetCDF CF

2.3 Pre-Processing

All

Preprocessing covers the preparation of the data so that they can be used for the classification. The Pre-processing block is composed of three major functions:

- Geo-referencing
- Topographic radiometric normalisation

The AATSR sensor is prone to aging and other effects that led to gradual changes in the data. These effects are compensated for by a **trend compensation** procedure by Dave Smith/RAL (<http://www.aatsrops.rl.ac.uk/EDSX/OtherInfo/>). RAL provides ENVI/IDL SW for the application of RAL's drift model, which was used within the SE prototype. Later that procedure was implemented in the SE processing system and follows the instructions by Smith and Caroline Poulsen "How to Apply the AATSR VIS-SWIR Calibration Corrections" (<http://www.aatsrops.rl.ac.uk/EDSX/OtherInfo/>).

The **geo-referencing** (including correction for topographic effects) may be done by ESA's BEAM software (<http://www.brockmann-consult.de/cms/web/beam/>) package, which is already tailored to ATSR-2 and AATSR data. The relevant BEAM functionality can be run in batch mode in this processing system. The orthorectification implementation is described in <http://www.brockmann-consult.de/beam/doc/help/visat/OrthorectificationAlgo.html> that is

based on the MERIS Geometry Handbook by Riazanoff (2005). The recommended procedure to geolocate A/ATSR data based on the Geolocation GRID provided within the AATSR data is described in the AATSR manual and the corresponding FAQ

(http://envisat.esa.int/instruments/aatsr/faq/#_Ref122167576). These recommendations as well as the MERIS manual are reference documents for the orthorectification procedure in the processing system that replaces the BEAM package. For orthorectification both modules, the BEAM package as well as the GS PS ortho modules rely on the GETASSE30 DEM. In particular the version provided by Brockmann

(<http://www.brockmann-consult.de/beam/doc/help/visat/GETASSE30ElevationModel.html>)

Topographic radiometric effects could strongly affect the FSC retrieval result if not corrected for in mountainous regions. For **topographic radiometric correction** ('terrain normalisation') C-correction is applied. Teillet et al. (1982) developed this semi-empirical method based on a modified variant of the cosine correction in their attempt to correct for topographic effects that could not be overcome by means of the conventional cosine correction method. Later called 'the C-correction method' by Meyer et al. (1993), this methodology has been used extensively by many researchers. Teillet et al. (1982) incorporated in its formulation a semi-empirical parameter (C) obtained from the satellite data to be corrected:

$$L_h = L_t \frac{\cos \theta_z + C}{\cos \theta_t + C} \quad (2.3.1)$$

where L_h is the calculated radiance for a horizontal surface, L_t is the observed radiance over the terrain, θ_z is the solar zenith angle and θ_t is the solar incidence angle to the local terrain normal. The C-correction may be interpreted as a correction for the effects of the atmospheric upwelling path radiance and the downward sky diffuse irradiance. Meyer et al. (1993) noted that the incorporation of the C parameter in the formulation tends to significantly reduce the overcorrection of data, especially for slopes facing away from the sun, as compared to the traditional cosine-correction based approaches.

We have determined a generally optimal value for C by testing for a range of C values and comparing FSC retrieval results to accurate reference snow maps based on Landsat TM. The value of C was varied from 0.005 to 0.5. The RMS error was calculated in each case. It was found that the sensitivity was quite small for a range of C -values (0.01–0.1). $C = 0.05$ has been chosen as a generally optimal and rather robust value (due to the low sensitivity in the range around that value).

Digital Elevation Model is applied in geo-referencing and radiometric topographic correction. Here GETASSE30 DEM is used, (<https://earth.esa.int/services/amorgos/download/getasse/> and <http://www.brockmann-consult.de/beam/doc/help/visat/GETASSE30ElevationModel.html>).

The decomposition of Pre-processing is illustrated in the diagram in Figure 2.3.1.

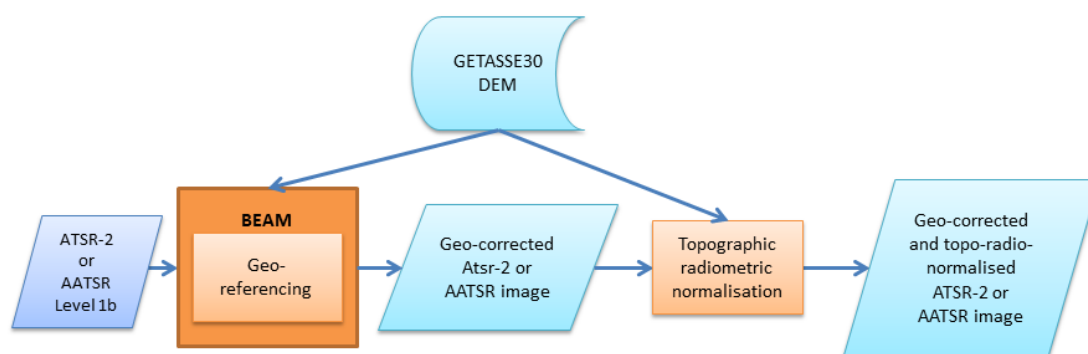


Figure 2.3.1 Decomposition of Pre-processing.

2.4 Cloud Detection

Sari Metsämäki

Several cloud detection methods for optical remote sensing data have been developed. Typically these are based on hierarchical decision rules and thresholding (Ackerman et al., 1998; Gesell, 1989; Irish et al., 2006; Khlopenkov et al., 2007; Knudby et al., 2011; Saunders and Kriebel, 1988). A lot of effort has been put to snow/cloud discrimination, but problem still remain not solved. Particularly the cloud/snow confusion causing false cloud commissions at the edges of snow-cover is a problem (Hall et al. 2007; Solberg et al., 2010). Such false commissions reduce the data usable for snow mapping. Since AATSR operational cloud mask was found to have difficulties over snow-covered terrain, a new cloud screening method applicable to AATSR was established for generation of GlobSnow SE v1.2. Since it was found by that improvements for cloud scening were still necessary, a new cloud screening method SCDA2.0 was developed and implemented for SE v2.0 processing chain. SCDA2.0 was designed to be used for optical and infrared data by sensors such as Terra/MODIS, ERS-2/ATSR-2, ENVISAT/AATSR, NPP Suomi/VIIRS and Future Sentinel-3 SLSTR. The method uses wavelength bands that are common for these sensors but not all of them, due to requirement of simplicity and low computing costs. Bands 550 nm, 1.6 μm , 3.7 μm , 11 μm and 12 μm were chosen.

The methodology is based on the several empirically determined decision rules, determined from selected training areas representing (by visual judgement) clouds, snow-covered terrain, partially snow-covered terrain and snow-free terrain. NPP Suomi/VIIRS and Terra/MODIS data from several dates and from different regions over Northern hemisphere provided the training data. The decision rules were determined as a heuristic approach by investigating the distributions of features – reflectances, brightness temperatures and their-related ratios - in different projections. Figure 2.4 presents the resulting cloud screening scheme. It should be noted that the success of cloud screening is based on visual evaluation on several (other than training data) MODIS, VIIRS and AATSR acquisitions, i.e. no *in situ* cloud observations were used for assessments. Instead, comparison against cloud mask provided with MOD10_L2 fractional snow product was made for several MODIS swaths particularly for acquisitions made during snow melt period.

The development work for SCDA2.0 was particularly targeting at identification of clouds throughout potential snow season for such regions where snow events are typical. Identification of clouds over regions without even ephemeral snow is therefore left without specific attention, which means that thin semi-transparent clouds over confident snow-free areas are not masked

2.5 Fractional Snow Cover Retrieval Algorithm

Sari Metsämäki

The FSC-retrieval block uses the *SCAmod* algorithm by Metsämäki et al. (2005; 2012).

The semi-empirical reflectance model-based method *SCAmod* originates from radiative transfer theory and describes the scene-level reflectance as a mixture of three major constituents – opaque forest canopy, snow and snow-free ground, which are interconnected through *apparent forest transmissivity* and the snow fraction. Transmissivity, in turn, can be derived from reflectance observations under conditions that highlight the presence of forest canopy – namely in the presence of full snow cover on the ground. Thus, *SCAmod* requires *a priori* information on transmissivity, but given that it can be determined with the appropriate accuracy, it enables the consideration for the obstructing effect of forests in fractional snow estimation.

SCAmod expresses the observed reflectance as follows:

$$\rho_{\lambda,obs}(FSC) = (1-t_{\lambda}^2) * \rho_{\lambda,forest} + t_{\lambda}^2 * [FSC * \rho_{\lambda,snow} + (1-FSC) * \rho_{\lambda,ground}] , \quad (2.5.1)$$

where $\rho_{\lambda,snow}$, $\rho_{\lambda,ground}$ and $\rho_{\lambda,forest}$ are the reflectances of snow, snow-free ground and forest canopy at wavelength λ , respectively. $\rho_{\lambda,obs}$ stands for the observed reflectance from calculation unit area. t_{λ}^2 stands for the apparent two-way transmissivity for the unit area.

In GlobSnow SE production, *SCAmod* employs top-of-atmosphere reflectance of AATSR Band 1 (545-565nm) as $\rho_{\lambda,obs}$, as delivered by the GlobSnow pre-processing module. The feasible values for the three reflectance constituents are based on NASA EOS Terra/MODIS-reflectance observations (top-of-atmosphere, from MOD02HKM) and field spectroscopy (Metsämäki et al., 2012, Heinilä et al., 2013; Salminen et al., 2009). These are as follows: $\rho_{\lambda,snow}= 0.65$, $\rho_{\lambda,forest}=0.08$ and $\rho_{\lambda,ground}$ is derived from spatially varying snow-free ground reflectance map (see Section 2.6). Optionally, a fixed value of $\rho_{\lambda,ground}=0.10$ can be applied, as in the case of v1.2 SE production.

FSC is then solved from (2.5.1) as follows:

$$FSC = \frac{\frac{1}{t_{\lambda}^2} * \rho_{\lambda,obs} + (1 - \frac{1}{t_{\lambda}^2}) * \rho_{\lambda,forest} - \rho_{\lambda,ground}}{\rho_{\lambda,snow} - \rho_{\lambda,ground}} . \quad (2.5.2)$$

SCAmod may result to $FSC > 1$ (100%) if the observed reflectance is higher than the maximum allowed by the model. This may be due to the nonrepresentative transmissivity or, more likely, due to the prevailing snow reflectance higher than expected (i.e. > 0.65). This is the case e.g. for dry snow introducing higher reflectance than that of melting (wet snow). The solution is to cut it to 1 (100%) (with the assumption that fractional snow is always wet):

$$\text{IF } FSC > 1 \text{ THEN } FSC = 1. \quad (2.5.3)$$

SCAmod may result to $FSC < 0$ if the observed reflectance is lower than the minimum assumed by the model. This may be due to e.g. very dense forest with shadows, or, due to snow-free terrain introducing true snow-free ground reflectance lower than the applied value of $\rho_{\lambda,ground}$. In this case, FSC is set to zero:

IF $FSC < 0$ THEN $FSC = 0$. (2.5.4)

Since SCAMod reflectance model relies on the observed reflectance alone, a separate test for identification of snow-free conditions has to be applied in order to avoid false snow detection if reflectance is increased due to another reason than snow. Normalized Difference Snow Index (NDSI) is used to identify snow-free cases. A threshold of -0.02 is used in GlobSnow. This threshold was empirically derived from NDSI-observations from Terra/MODIS imagery over Finland, using weather station data and information on general climatology to verify snow-free conditions soon after snow disappearance.

IF $NDSI < -0.02$ THEN $FSC = 0$. (2.5.5)

SCAMod accounts for the effect of forest canopy into the observed reflectance, provided that the *a priori* information on canopy transmissivity is available. This is the challenge of using the model – but the solution is provided by the model itself. Namely, according to (2.5.1), if ground layer is 100% snow covered (i.e. $FSC=1$), the observed reflectance originates only from forest canopy and snow. Consequently, two-way transmissivity t^2 can be solved from the observed reflectance as follows:

$$t_{\lambda}^2 = \frac{\rho_{\lambda,obs}(FSC=1) - \rho_{\lambda,forest}}{\rho_{\lambda,snow} - \rho_{\lambda,forest}}. \quad (2.5.6)$$

Transmissivity is traditionally generated using reflectance observations acquired at full snow cover conditions (Metsämäki et al. 2005 and 2012). While doing this, generally applicable reflectance from dry snow is used in order to reduce the fluctuations caused by varying grain size and impurities. Thus $\rho_{\lambda,snow} = 0.84$ in Eq. (2.5.6), based on sampling on representative MODIS observations. For transmissivity calculations, NASA EOS Terra/MODIS TOA-reflectances have been used due to the good spatial and temporal coverage and availability of the data.

The generally applicable value for **snow reflectance** $\rho_{\lambda,snow}$ in eq. (2.5.1) is empirically derived from i) MODIS band 4 reflectance observations from snow-covered non-forested areas (Metsämäki et al., 2012) and ii) at-ground spectral measurements conducted in Finland (Salminen et al., 2009; Niemi et al., 2012). For the latter, conversion from at-ground reflectance to top-of-atmosphere reflectance was conducted using the Simplified Method for Atmospheric Correction (SMAC) (Rahman and Dedieu (1994); Berthelot, 2003) with standard atmosphere adjusted to Finnish springtime conditions. It is recognized that using only one value for snow reflectance does not respond to the large variation of snow reflectance caused by varying grain size, impurities and thickness (e.g. Dozier et al., 2009; Nolin and Dozier, 2000; Painter and Dozier, 2004; Warren; 1982). In provision of GlobSnow SE, these variances are propagated in the uncertainty of FSC (see Section 2.7), while the applied constant value ($\rho_{\lambda,snow}=0.65$) is considered a feasible approximation for the average case.

Forest canopy reflectance $\rho_{\lambda,forest}$ in eq. (2.5.1) refers to totally opaque forest canopy. Since such canopies are not easy to identify, we have to rely on observations from canopies we assume are close to opaque. The applied value was mainly derived from MODIS reflectance observations from carefully selected very dense boreal forests over Finland and Russia (Metsämäki et al., 2012), but also from reflectance measurement of thick layers of Scots pine branches at laboratory conditions (Niemi et al., 2012). Value of 0.08 for $\rho_{\lambda,forest}$ is considered feasible for FSC estimation.

2.5.1 Hemispheric transmissivity generation

Sari Metsämäki

In hemispherical scale, generation of transmissivity using MODIS (or any other) reflectance observations would be far too laborious and in some areas even impossible to implement due to the lack of representative cloud-free data. Therefore, the global transmissivity is generated using global landcover data and their-related transmissivity statistics. Investigation on the correspondence between existing transmissivity data (based on MODIS-reflectance data) and the GlobCover data (*GlobCover Land cover v2 2008, regional product*, Bicheron et al., 2008) yielded an average transmissivity for each GlobCover class. This information was the used to generate transmissivity map for the entire GlobSnow geographical domain.

In order to relate the GlobCover (GC) classes and their representative transmissivity, the class-stratified mean and standard deviation of transmissivity was determined using the already existing MODIS reflectance-derived transmissivity data over several training areas over the Northern Hemisphere. In the analysis, the transmissivity data had a resolution of $0.01^\circ \times 0.01^\circ$, while GlobCover data was processed into a resolution of $0.0025^\circ \times 0.0025^\circ$. These two were go-registered so that each GlobSnow pixel matches with 4×4 GlobCover pixels. Whenever a clear majority of pixels introduced a one specific class, the transmissivity value was taken into statistical database. From the database, the mean and standard deviation for each class was determined. After this was finalized, the transmissivity for each $0.01^\circ \times 0.01^\circ$ pixel of the whole target area can be expressed as a linear combination of class-wise average transmissivity and the class-wise occurrence of GlobCover pixels (4×4) falling into that pixel, as follows:

$$transmissivity_{i,j} = \sum_{c=1}^{N_{classes}(i,j)} \frac{n_{c,i,j}}{n_{tot,i,j}} * mean(t_{MODIS}(c)), \quad (2.5.7)$$

where i,j are grid cell coordinates (cell size $0.01^\circ \times 0.01^\circ$)
 $n_{c,i,j}$ is number of GlobCover pixels of class c in within a grid cell i,j
 $n_{tot,i,j}$ is total number of GlobCover ($0.0025^\circ \times 0.0025^\circ$) pixels within grid cell (=16)
 $mean(t_{MODIS}(c))$ is the mean transmissivity for class c
 $N_{classes}(i,j)$ is the number of GlobCover classes within cell i,j .

For v1.2 SE production in GlobSnow-1, transmissivities needed for statistical analysis were first derived from MODIS-acquisitions for five extensive training areas in the Northern Hemisphere, together compounding an area of ~ 7 million km^2 . For each area, transmissivity distributions (mean and standard deviation) were determined for present GlobCover-classes and then combined after normalizing with respect to the size of a training area. An example of distributions for two classes is presented in Figure 2.5.1. In general, GlobCover classes are rather well separated with respect to their typical average transmissivity, although some classes exhibit a large standard deviation and their distributions were overlapping. There are also differences between the teaching areas. Nevertheless, it was considered reasonable to determine the continental transmissivity maps using GlobCover data and these averages. The feasibility of this approach was later verified simply by comparing the original MODIS-derived transmissivity (referred to as $trans_{MODIS}$) and the new GlobCover-derived transmissivity ($trans_{GC}$), see Metsämäki et al., (2012).

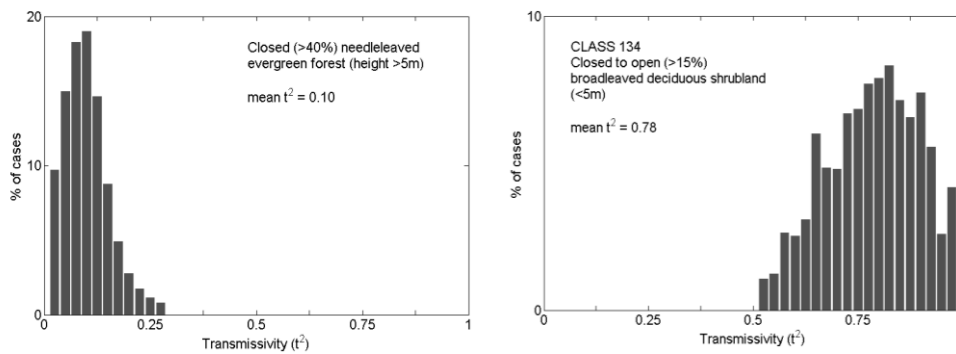


Figure 2.5.1 Examples of GlobCover class-related distribution of MODIS-derived transmissivity for one of the training areas, *Left*: class 70, *Right*: class 134.

The analyses for v1.2 SE product exploiting the continental-scale transmissivity map within GlobSnow-1 revealed that the proposed approach for transmissivity generation did not fully catch the densest forest, i.e. too high transmissivities were often obtained compared to original MODIS-derived values. Also high transmissivities were not properly caught. This evidently had implications to fractional snow cover estimates. For dense forests, this was seen as underestimations of FSC, and for open areas, as overestimations. The analysis on the spatial patterns of discrepancies between $trans_{GC}$ and $trans_{MODIS}$ revealed that most problems occurred with four particular boreal forest classes (50, 90, 92, 100; see Bicheron et al. (2008) its Appendix II). In continental-scale GlobCover-data, these classes appear to represent both very dense and moderate dense forests, implying that a wide distribution of transmissivities is assigned to each of these classes in the training areas. As a result, the gained average transmissivity did not properly represent either of the forest types. So it was found very likely that the GlobCover-based approach would benefit from external data accounting for the forest density.

Compared to other land covers, *albedo* from boreal forest is low throughout the year, but the contrast in winter is even larger. Although there is an increase in albedo over snow-covered boreal forests (snow on or below the canopy), these albedos clearly differ from those from non-forested areas (Betts and Ball, 1997; Barlage et al., 2005; Moody et al. 2007). Hence it was decided to test the feasibility of wintertime global albedo-data in discriminating between moderate and dense forests. According to Manninen and Stenberg (2009), red-band albedo from snow-covered (snow below the canopy) boreal forest is dominated by the bidirectional transmissivity to and from the forest floor, while NIR-albedo is predominantly contributed by canopy scattering (direct or after interacting with the forest floor). Hence, visible albedo was considered to have the best correlation with transmissivity and therefore should be the best candidate in identification of the most dense forests. Here white-sky albedo was chosen as it is independent on the angular effects. Finally, the ESA GlobAlbedo (Müller et al. 2012) white-sky visible albedo from two 8-day composites (March22 and March30 2005 for Eurasia; Feb26 and March06 2005 for Northern America; minimum of these is chosen to diminish the effect of snow-on-tree canopy) was used in identifying the densest forests. The albedo in $0.05^\circ \times 0.05^\circ$ grid were resampled into $0.01^\circ \times 0.01^\circ$ grid to be compatible with GlobSnow processing grid.

The analysis between the albedo – with snow cover on terrain prevailing – showed that there is a high linear correlation between the albedo and MODIS-derived transmissivity particularly at very low transmissivity and albedo. Hence it was concluded that the specified four GlobCover forest classes can be divided into two sub-classes, moderate and dense, according to their albedo. The threshold for judging between these two was set to 0.15, based on results by Betts and Ball (1997) as well as on empirical tests with $trans_{MODIS}$ and Global albedo data. The

corrections to continental transmissivity map was carried out for pixels dominated by one of the four classes or mixture of them and at the same time, showing albedo less than the threshold i.e. representing dense forest. The linear fitting parameters gained from the above described analysis was applied to decrease the original transmissivity relative to the albedo. It should be noted that this technique is valid only in the presence of full snow cover, correspondingly to transmissivity calculations as presented in Metsämäki et al., (2005, 2012). Therefore, snow information from global GlobSnow Snow Water Equivalent (SWE) product (Takala et al., 2011) from was used to identify the snow-covered areas before launching the procedure. The applied SWE-data were March30 2005 for Eurasia and March06 2005 for North America. The SWE-data were processed into GlobSnow 0.01°×0.01° grid.

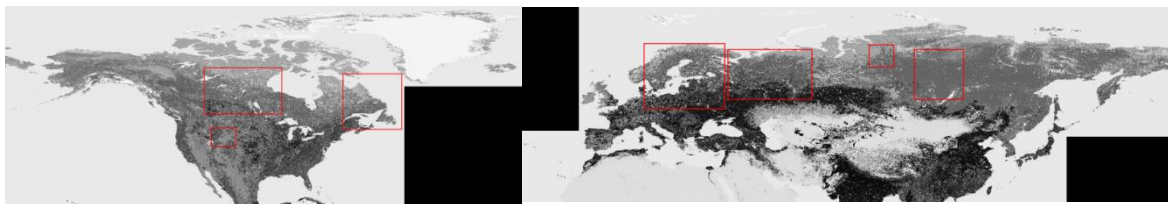


Figure 2.5.2 Training areas for Northern Hemisphere transmissivity determination using MODIS-derived transmissivities and GlobCover-data.

To update the continental transmissivity map for GlobSnow v2.0 SE production, also the number of training areas was increased to seven in order to obtain a large number of samples and thus more reliable statistics for each relevant GlobCover class. This extension resulted in transmissivity training area 10 million km².

The new two-way transmissivity maps for Eurasia and North America are presented in Figure 2.5.3. Compared to the GlobSnow-1 transmissivity, the new maps show significant decrease of transmissivity values over boreal forest areas, e.g. for needleleaved deciduous forests in Siberia. Also many local changes towards lower transmissivity over very dense forests in Russia are found. It is very likely that the new map better responses to the different densities of the four forest classes.

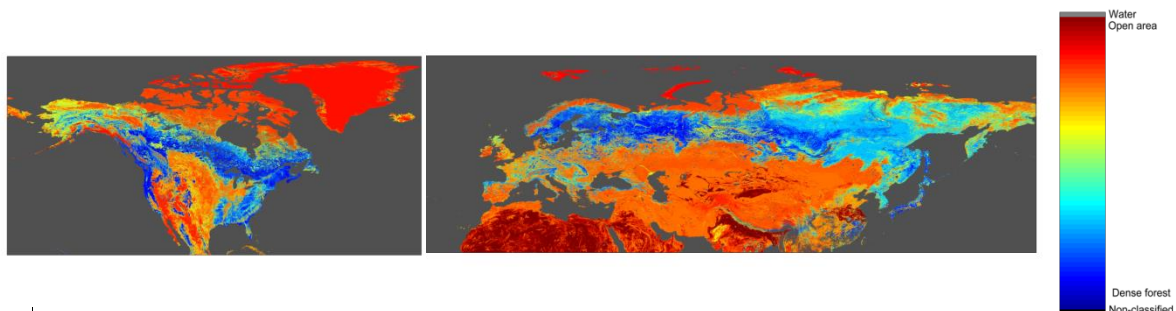


Figure 2.5.3 Transmissivity map for Eurasia (top) and North America (bottom).

2.6 Snow-free ground reflectance map

2.6.1 Snow-free ground reflectance map for plains

Miia Salminen & Sari Metsämäki

SCAmod features snow-free ground reflectance as one of the model parameters (eq. 2.5.1 and 2.5.2). The success of FSC estimation therefore depends on the representativeness of the applied value for $\rho_{l,ground}$. The earlier GlobSnow v1.2 SE implementation of SCAmod uses a fixed value $\rho_{l,ground} = 0.10$ (10%) at the visible wavelengths around 555 nm, corresponding to AATSR band 1 and MODIS band 4. In practice, the spatial and temporal variability of $\rho_{l,ground}$ causes an error contribution to FSC estimation. For v2.0 SE production this variability was considered by determination of post-winter snow-free ground reflectance statistics to be applied by SCAmod as auxiliary data. For seasonally snow-covered areas in the Northern Hemisphere, the snow-free ground (mean and variance) reflectance map was determined using reflectance time-series and land cover information (ESA GlobCover data). From the time-series, the observations representing (post-melt) snow-free ground situation were extracted using the methodology by Salminen et al., (2013). The extracted pixel-wise values and GlobCover-data were then used to generate class-stratified snow-free ground reflectance statistics, which were applied in generating the snow-free ground reflectance map. For generation of time-series, reflectance acquisitions by Terra/MODIS were selected due to this sensor's good spatial and temporal coverage compared to those of AATSR; it operates at the corresponding wavelength bands and is therefore suitable to represent AATSR for this purpose. The swath level MOD02HKM data were calibrated to top-of-atmosphere reflectances and processed into 0.005° geographical grid. For regions with ephemeral snow, the snow-free ground reflectance statistics were determined by analyzing selected regional or global MOD09 products, i.e. calculating reflectance statistics for the valid land cover types. This was accomplished for GlobCover bare ground classes using test regions from Sahara (consolidated bare areas), Aral Sea (salt hardplains and bare areas) and Taklamakan desert (sandy desert).

The time-series based methodology was first developed by using a test area covering Central, Eastern and Northern Europe and for various land cover categories by applying ESA GlobCover data as reference (Salminen et al., 2013). The time-series analysis was conducted for 8 land cover classes (Salminen et al. 2013), the total analyzed surface area being 583 km². For v2.0 SE production, the method was applied also for a test area from North America, where the analysed surface area is 3176 km², within latitudes N50°- N65° and longitudes W90°- W115°. For North America, the time-series analysis was performed for 4 land cover classes not analyzed in European training area; for other classes, snow-free ground reflectance were derived from European training area. Also Eurasian snow-free ground reflectance map is based on the analyses made for European training areas. Overall, forested classes are assigned a value of 0.10 (10%) for snow-free ground reflectance.

The number of samples for different GlobCover classes varies according to their occurrence in the training areas. Therefore, not all GlobCover classes were analysed with the same thoroughness; but once established, the method can be gradually applied to other test areas to encompass all relevant classes present in seasonally snow-covered areas in the Northern Hemisphere. The current established snow-free ground reflectance map features ρ_{ground} values that vary spatially according to land cover class in the entire GlobSnow geographical domain. However, some classes are assigned with $\rho_{l,ground}$ from another nearly corresponding class. And, as mentioned above, forested areas retain a fixed value of 0.10 (10.0 %) since these were not

included in the analyses. The procedure for obtaining the snow-free reflectance map for plains is depicted in Fig 2.6.1.

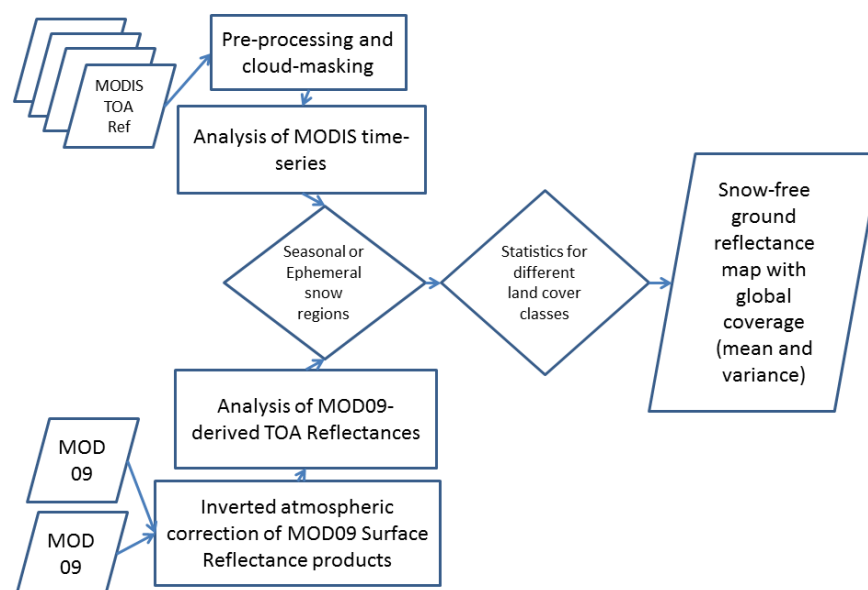


Figure 2.6.1 An overview of the procedure for the determination of the (static) map of snow-free ground reflectance (and its variance). In regions of seasonal snow cover, an analysis of MODIS time-series is carried out in order to extract the values of surface reflectance immediately after the snow melt. In other regions (bare surfaces) snow-free ground reflectance is estimated from the statistics of MOD09 surface reflectance products.

The key question in the time-series analysis is to find the valid reflectance observation representing the snow-free conditions right after the last traces of snow have disappeared. This value is then assumed to represent snow-free ground reflectance during the actual ablation season, prior to the appearance of the green vegetation. This assumption is based on the earlier investigations e.g. (Stow et al., 2004), reporting that green vegetation – shown as increasing reflectances and particularly NDVI – appears only after the final snow clearance. The obtained feasible ρ_{ground} -values from all the selected pixels and their class-wise variability information can be exploited in generating a ρ_{ground} map and, further, in the accuracy assessment of FSC estimation for each land cover class.

The class-stratified snow-free ground reflectance values obtained from the European test area are listed in Tables 2.6.1 and 2.6.2. As indicated in Table 2.6.3, the analysed GlobCover classes cover almost all of the open and sparsely forested areas of the European test region. For those classes remained not analysed, value from the closest resembling class is given (see Table 2.6.4). Exceptions are bare ground classes 200, 201, 202 and 203, for which the representative value (mean and standard deviation) was derived from MOD09 surface reflectance data. MOD09 surface reflectances were converted to TOA reflectances by applying MODTRAN (Anderson et al., 1995; Berk et al., 1989) simulations of a standard continental atmosphere. All the resulting reflectance values were employed in the determination of northern hemisphere snow-free ground reflectance map. The map for the European test area is shown in Fig 2.6.2. The final ρ_{ground} information for Eurasia and North America is illustrated in Figure 2.6.3.

Table 2.6.1 Snow-free ground reflectance statistics for GlobCover classes: Agricultural areas/steppe (20), Tundra/Sparse vegetation (150) and Wetlands (180). Mean, Standard Deviation (SD) and Number of observations. Mean and SD are accompanied by their confidence intervals.

	<i>t² > 0.5 and time window maximum of 15 days after snow clearance</i>									
	Class 20 (N obs 495)		Class 180 (N obs 421)		Class 150 (N obs 728)		Class 150 Tundra (N obs 329)		Class 150 Sparse (N obs 399)	
Criteria	Mean (± 95% conf.)*	SD** (95% bounds)	Mean (± 95% conf.)*	SD** (95% bounds)	Mean (± 95% conf.)*	SD** (95% bounds)	Mean (± 95% conf.)*	SD** (95% bounds)	Mean (± 95% conf.)*	SD** (95% bounds)
MODIS 4	10.01 (0.12)	1.34 (1.26, 1.43)	7.38 (0.07)	0.75 (0.70, 0.80)	10.02 (0.16)	2.16 (2.05, 2.28)	10.09 (0.30)	2.73 (2.64, 2.96)	9.96 (0.15)	1.53 (1.43, 1.64)

* 95% ± confidence interval

**SD = standard deviation; lower and upper bounds for the 95% confidence interval

Table 2.6.2 Snow-free ground reflectance statistics for GlobCover classes: Rainfed croplands (14), Mosaic vegetation/cropland (30), Mosaic forest or shrubland/grassland (110) and Closed grassland (141). Mean, Standard Deviation (SD) and Number of observations. Mean and SD are accompanied by their confidence intervals.

	<i>t² > 0.5 and time window maximum of 15 days after snow clearance</i>							
	Class 14 (N obs 398)		Class 30 (N obs 127)		Class 110 (N obs 52)		Class 141 (N obs 110)	
Criteria	Mean (± 95% conf.)*	SD** (95% bounds)	Mean (± 95% conf.)*	SD** (95% bounds)	Mean (± 95% conf.)*	SD** (95% bounds)	Mean (± 95% conf.)*	SD** (95% bounds)
MODIS 4	10.68 (0.11)	1.07 (1.00, 1.15)	8.94 (0.44)	2.49 (2.21, 2.84)	10.41 (0.44)	1.58 (1.33, 1.96)	11.13 (0.43)	2.28 (2.01, 2.63)

* 95% ± confidence interval

**SD = standard deviation; lower and upper bounds for the 95% confidence interval

Table 2.6.3. The surface area of all the non-forested and sparsely forested classes with the obtained time series-based snow-free ground reflectance in the European test area. The surface area is also presented for classes which remained without a specifically analysed snow-free ground reflectance, and thus obtain the value from other classes or are assigned the fixed value of 10.0 % as applied in v1.2 SE production.

GC Class	Class Group Title	Surface area (%)*	Class description based on Bicheron et al. (2008)
20, 150, 180, 14, 30, 110, 141	Open/non-forested area classes with the obtained Snow-free ground reflectance	48.80	Non-forested and sparsely forested areas (excluding urban areas, bare areas and permanent snow and ice)
13, 15, 16, 21, 32, 120, 140, 151, 152, 185, 190, 201, 202, 203, 220	Other open/non-forested area classes with no new Snow-free ground reflectance	3.89	Non-forested and sparsely forested areas (including urban areas, bare areas and permanent snow and ice)
200	value from the closest resembling class is used, see Table 2.6.4 value derived from MOD09 from representative area		
50, 60,70, 90, 91, 92, 100, 101, 130, 131, 134	Forested classes (constant prefixed value is used)	46.38	Consisting of various broadleaved and needleleaved forests and (closed) shrublands

* % of the total surface area of all classes excluding water bodies

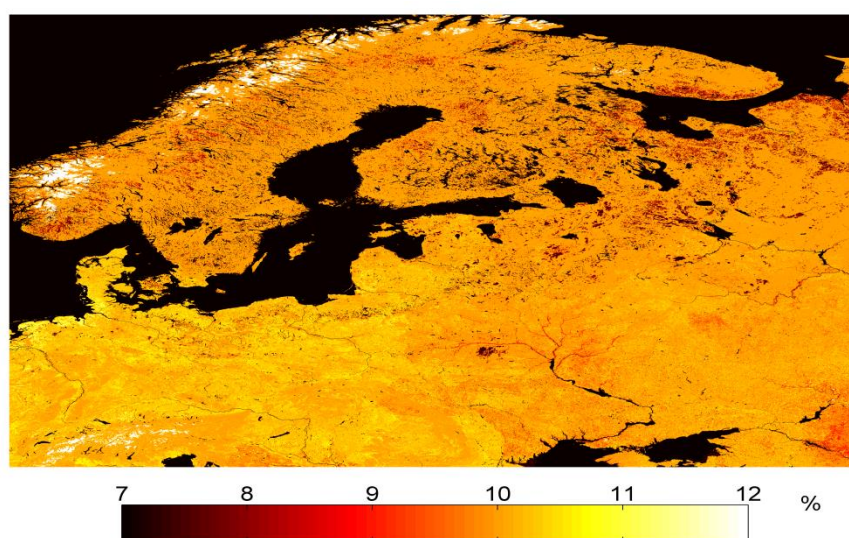


Figure 2.6.2 Retrieved map of TOA-reflectance of snow-free ground at the MODIS band 4 (545-565 nm) covering the Central, Eastern and Northern European test area. Ice caps are shown by white color; their reflectance is much higher than the image threshold value of 12%.

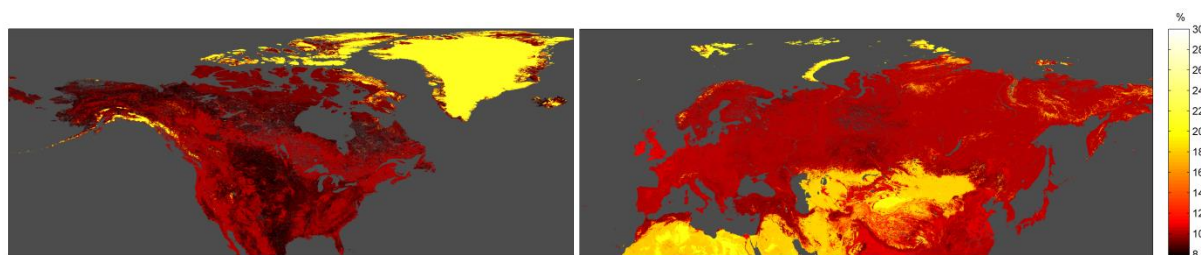


Figure 2.6.3. The snow-free ground map for Eurasia (top) and North America (bottom).

Table 2.6.4. Generalization of investigated GlobCover classes to correspond to non-investigated classes, for merging of snow-free ground reflectance statistics (mean and standard deviation for Eurasia).

GC Class	In agreement with	Mean	Standard deviation	Class description based on Bicheron et al. (2008)
20	21, 22	10.01	1.34	Mosaic cropland (50-70%) or other vegetation (20-50%)
150	151, 152, 153, 120	10.02	2.16	Sparse (>15%) vegetation (woody vegetation, shrubs, grassland)
180	181, 182, 183, 184, 185, 186, 187, 188	7.38	0.75	Closed to open (>15%) grassland or woody vegetation on a regularly flooded or waterlogged soil, also with fresh, brackish or saline water
14	11, 12, 13, 15, 16	10.68	1.07	Rainfed croplands
30	31, 32	8.94	2.49	Mosaic vegetation (50-70%) / cropland (20-50%)
110	-	10.41	1.58	Mosaic forest or shrubland (50-70%) / grassland (20-50%)
141	140, 142, 143, 144, 145	11.13	2.28	Closed (>40%) grassland (Sub-class of 140, which is closed to open (>15%) herbaceous vegetation)
Forested classes	40, 41, 42, 50, 60, 70, 90, 91, 92, 100, 101, 102, 130, 131, 132, 133, 134, 135, 136, 160, 161, 162, 170	not obtained (use 10.0)	1.5	Forested classes including closed shrublands
190	-	10	1	Artificial surfaces and associated areas (Urban areas >50%)
200	200 201 202 203	18.37 17.84 20.31 32.75	1.36 3.58 0.82 2.79	Bare areas (consolidated and non-consolidated)
210	-	3.00	1	Water bodies
220	-	21.00	1	Permanent snow and ice
230	-	10.00	1	Error in GlobCover data

Table 2.6.5. Generalization of investigated GlobCover classes to correspond to non-investigated classes, for merging of snow-free ground reflectance statistics (mean and standard deviation for North America).

GC Class	In agreement with	Mean	Standard deviation	Class description based on Bicheron et al. (2008)
20	21, 22	10.01	1.34	Mosaic cropland (50-70%) or other vegetation (20-50%)
150	151, 152, 153	9.28	1.39	Sparse (>15%) vegetation (woody vegetation, shrubs, grassland)
120	-	7.80	0.81	Mosaic grassland (50-70%) / forest or shrubland (20-50%)
180	181, 182, 183, 184, 185, 186, 187, 188	7.38	0.75	Closed to open (>15%) grassland or woody vegetation on a regularly flooded or waterlogged soil, also with fresh, brackish or saline water
14	11, 12, 13, 15, 16	10.68	1.07	Rainfed croplands
30	31, 32	8.94	2.49	Mosaic vegetation (50-70%) / cropland (20-50%)
110	-	7.89	0.93	Mosaic forest or shrubland (50-70%) / grassland (20-50%)
140	141, 142, 143, 144, 145	7.91	0.93	Closed to open (>15%) herbaceous vegetation (grassland, savannas or lichens/mosses)
Forested classes	40, 41, 42, 50, 60, 70, 90, 91, 92, 100, 101, 102, 130, 131, 132, 133, 134, 135, 136, 160, 161, 162, 170	not obtained (use 10.0)	1.5	Forested classes including closed shrublands
190	-	10	1	Artificial surfaces and associated areas (Urban areas >50%)
200	200 201 202 203	18.37 17.84 20.31 32.75	1.36 3.58 0.82 2.79	Bare areas (consolidated and non-consolidated)
210	-	3.00	1	Water bodies
220	-	21.00	1	Permanent snow and ice
230	-	10.00	1	Error in GlobCover data

2.6.2 Snow-free ground reflectance map for mountains

Rune Solberg and Øivind Due Trier

The main objective of this study has been to determine top-of-atmosphere reflectance values, representative of mountain land cover types, which can be used for snow-free ground reflectance parameterisation in the Snow Extent snow retrieval algorithm. The snow-free ground reflectance values we seek are those present under fractional snow cover conditions. This is done by retrieving snow-free ground reflectance values as soon as the snow has melted.

In mountainous regions the snow may melt over a very long period determined by local snow accumulation conditions (depending on precipitation and wind), exposition, elevation range and weather (mainly wind and temperature). For some mountainous regions the snowmelt might take place over up to half a year. To establish the snow-free ground reflectance pixel by pixel just after the snow has melted for a given mountain region, lots of satellite observations are needed.

To determine the time when the snow just has completely melted on a per pixel basis, we have used an algorithm developed by NR to analyse and interpret time series of reflectance observations. We here determine average reflectance for a selection of regions where the inter-region reflectance might differ due to different regional vegetation, geology and climate. The reflectance is further stratified into the dominating land cover classes for each region to cope for within-region variability. Four regions were chosen for the study: Scandinavian Mountains, Caucasus Mountains, Tibetan Plateau and Rocky Mountains.

Data set

The reflectance of the observed ground surface cover is mainly determined by the local geology/mineralogy, vegetation and soil moisture. Ideally, the reflectance should have been derived for all mountain regions where geology/mineralogy and vegetation cover differ significantly. However, the amount of data and processing needed is significant, and we chose as a compromise four regions representing significant diversity with respect to the three aspects. Also, for the same reasons, we could not map each mountain region to the full extent, so a representative sub-region was chosen with a suitable size relative to the coverage of the MODIS sensor (Table 2.6.6 and Figure 2.6.4).

Table 2.6.6 Geographic extent of the four study sites.

Geographic area	West	East	North	South
Scandinavian Mountains	4°30'	31°35'	71°30'	57°55'
Caucasus Mountains	37°	50°	45°	35°
Tibetan Plateau	80°	95°	45°	30°
Rocky Mountains	-114°	-104°	42°	32°



Figure 2.6.4 The four study sites covered with MODIS images superimposed on the GlobCover land cover map.

The MODIS MOD 02 Level-1B Calibrated Geolocation Data Set was applied for establishing the snow-free ground top-of-atmosphere (TOA) reflectance. The MOD 02 data set contains calibrated and geolocated at-aperture radiances for the 36 bands generated from MODIS Level-1A sensor counts (MOD 01). Reflectance was determined for the solar reflective band 4 at 555 nm (bandwidth 545–565 nm), which was applied here, through application of the solar irradiance, which is delivered with the data.

The land cover types were determined from the ESA GlobCover MERIS FRS 2009 mosaics (Bontemps et al., 2010). The global land cover map counts 22 land cover classes defined with the United Nations Land Cover Classification System (LCCS). The GlobCover 2009 land cover product is of 300 m resolution in the map projection Plate-Carrée (WGS84 geoid). For our application in GlobSnow the map has been resampled to a $0.01^{\circ} \times 0.01^{\circ}$ lat/lon raster map.

A mountain mask was created by ENVEO in the first part of the GlobSnow project (see Section 2.10). Mountainous regions were identified and mapped using a smoothed slope map derived from a digital elevation model. Mountains are here defined as terrain where the general local terrain slope $> 2^{\circ}$. For the purpose of reflectance map generation here, we split the mountains in the Northern Hemisphere into regions. An ID code unique to each region was applied in the revised mountain mask to assist the processing of each region separately.

Methodology

The main approach is to find the time of snow-free ground surface just after the snowmelt season per pixel and for those pixels determine the corresponding reflectance from MODIS data. NR has developed an algorithm for automated analysis of time series of reflectance to determine the local (per pixel) winter snow (apparent) reflectance value and the post-snow-season snow-free ground reflectance value (just after the disappearance of the snow). We have here applied the post-snow-season dates found by the algorithm with AVHRR data for selecting the corresponding MODIS data.

The main principles of the algorithm are based on detecting snow seasonality and, with support of potential strong vegetation seasonality, to determine representative values for high (snow) and low (snow-free ground) reflectance. The most responsive wavelengths to snow (VIS) and vegetation (NIR), or the indices NDSI and NDVI, are used to determine snow and vegetation seasonality, respectively.

The maximum stable apparent winter reflectance and the post-snow-season snow-free ground reflectance are determined by analysing the structure of the temporal reflectance function per pixel. Strong and weak snow seasonality are handled separately to identify the most likely

representative values. If snow seasonality is totally missing, there is probably no snow or very dense coniferous forest hiding the ground snow cover.

Based on the described mask defining the mountain regions to analyse, the GlobCover land cover map defining the classes to calculate reflectance statistics for and the map of post-snow-season snow-free ground reflectance appearance dates, corresponding MODIS measurements of top-of-atmosphere (TOA) reflectance can be identified at a per-pixel level. For topographic correction ('terrain normalisation') C-correction is applied, which is intentionally the same as used in GlobSnow.

Results

The reflectance statistics derived for the four mountain regions are presented in the following. Reflectance is given in the range [0.0, 1.0].

Scandinavian Mountains

The rectangle in Figure 2.6.5 shows the extent of the region which was analysed. The actual area analysed was the intersection of this rectangle and the mountain mask.

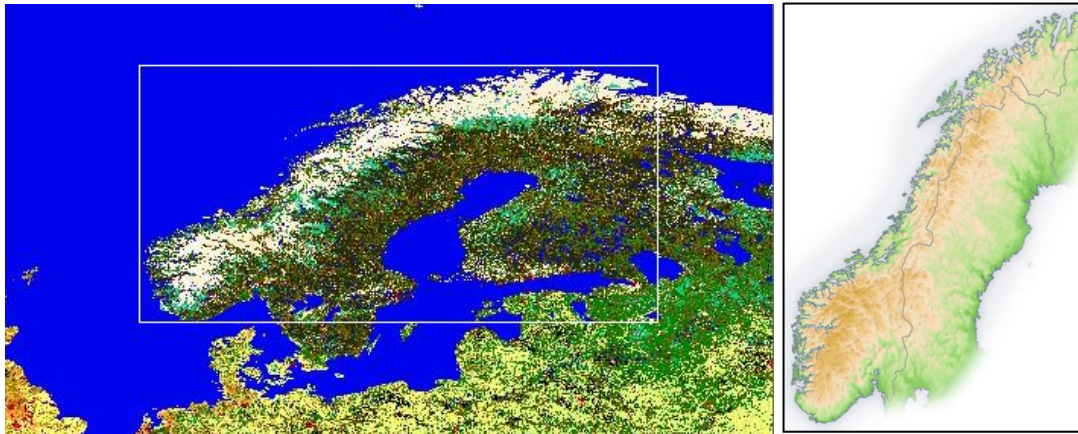


Figure 2.6.5 *Left*: The rectangle shows the Scandinavia Mountains domain defining the region of interest for the MODIS acquisitions with GlobCover 2009 as background map. *Right*: Elevation map for the Scandinavian Mountains.

Of the 22 GlobCover classes (see explanation in Table 2.6.7), a total of 18 is present in these mountains (we exclude class 230, 'no data'). Since the region is rich in moisture, the ground is in general covered by vegetation except for steep areas where the bedrock is exposed and where the ground is covered by large rocks draining loose material away. However, except for the tallest mountains even the rock surfaces are to a large degree covered with vegetation in the form of lichens.

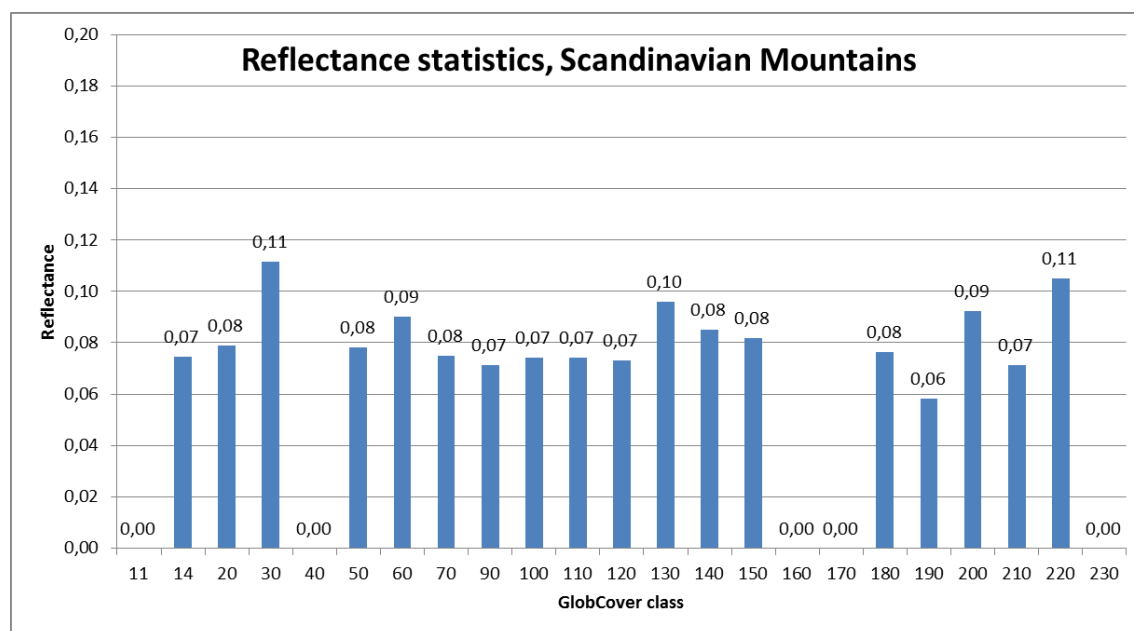


Figure 2.6.6 Reflectance statistics for the Scandinavian Mountains. The numbers along the X-axis are the GlobCover class numbers.

The reflectance range of the classes is relatively small, [0.06, 0.11], with an area-weighted mean of 0.079 (Figure 2.6.6). Note that class 210 (water bodies) and class 220 (permanent snow and ice) have been omitted when calculating the area-weighted mean. The main reason for the relatively small reflectance range is probably the domination of the vegetation cover, that most surfaces are covered by vegetation in one or another form. However, even the class “bare areas” (class 200) shows reflectance rather close to the mean (0.09), which is mainly determined by mineralogy and the presence of water (surface moisture).

Table 2.6.7 GlobCover class codes and explanation of classes.

Value	Explanation
11	Post-flooding or irrigated croplands (or aquatic)
14	Rainfed croplands
20	Mosaic cropland (50-70%) / vegetation (grassland/shrubland/forest) (20-50%)
30	Mosaic vegetation (grassland/shrubland/forest) (50-70%) / cropland (20-50%)
40	Closed to open (>15%) broadleaved evergreen or semi-deciduous forest (>5m)
50	Closed (>40%) broadleaved deciduous forest (>5m)
60	Open (15-40%) broadleaved deciduous forest/woodland (>5m)
70	Closed (>40%) needleleaved evergreen forest (>5m)
90	Open (15-40%) needleleaved deciduous or evergreen forest (>5m)
100	Closed to open (>15%) mixed broadleaved and needleleaved forest (>5m)
110	Mosaic forest or shrubland (50-70%) / grassland (20-50%)
120	Mosaic grassland (50-70%) / forest or shrubland (20-50%)
130	Closed to open (>15%) (broadleaved or needleleaved, evergreen or deciduous) shrubland (<5m)
140	Closed to open (>15%) herbaceous vegetation (grassland, savannas or lichens/mosses)
150	Sparse (<15%) vegetation
160	Closed to open (>15%) broadleaved forest regularly flooded (semi-permanently or temporarily) - Fresh or brackish water
170	Closed (>40%) broadleaved forest or shrubland permanently flooded - Saline or brackish water
180	Closed to open (>15%) grassland or woody vegetation on regularly flooded or waterlogged soil - Fresh, brackish or saline water

190	Artificial surfaces and associated areas (Urban areas >50%)
200	Bare areas
210	Water bodies
220	Permanent snow and ice
230	No data (burnt areas, clouds,...)

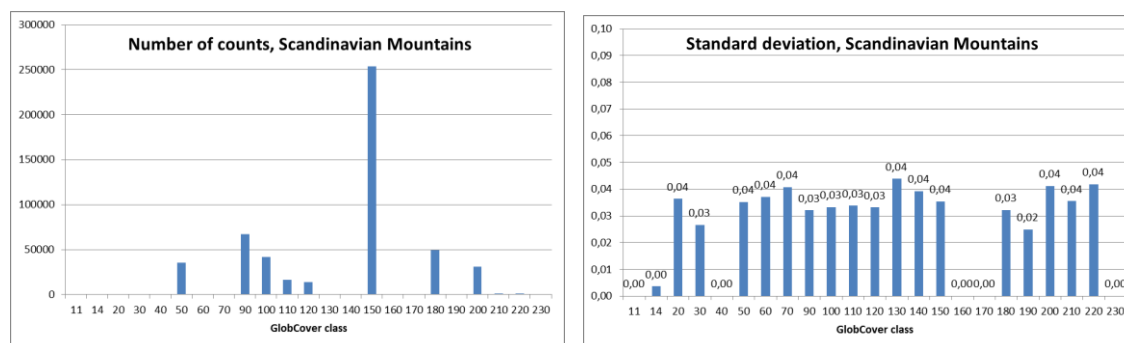


Figure 2.6.7 *Left*: Number of counts (observations) for the Scandinavian Mountains (corresponding to the data set in Figure 2.6.6). *Right*: Standard deviation for the reflectance of each class.

Class 150 (sparse vegetation) totally dominates the area (Figure 2.6.7, left). There are only seven other classes of significant dominance, with 50, 90 and 100 representing forest, 110 and 120 representing shrubland/grassland of various mixtures, 180 representing a mixture of grassland and trees, and 200 (adding to 150, sparse vegetation) with completely bare areas.

Since each ground point (pixel) is observed only once with the methodology used, the number of observations corresponds fairly well with the area distribution of the classes ('fairly' because in some cases the time of snow-free ground just after the snowmelt could not be determined using our methodology and therefore had to be discarded).

The classes exhibit quite significant reflectance variability (Figure 2.6.7, right). The typical standard deviation is 0.03 or 0.04, which corresponds to almost 50% of the mean reflectance value for several classes. This might not be surprising as the relatively few GlobCover classes represent a fairly significant level of land cover generalisation. The natural world usually exhibits quite a lot of variability. In addition to expected land cover variability, there is variability due to soil moisture and cast shadows, and it must be expected that there is variability in the vegetation's phenological development for otherwise similar observations.

Caucasus Mountains

The reflectance range of the classes is somewhat larger for the Caucasus Mountains than for the Scandinavian Mountains, [0.05, 0.14], but with an area-weighted mean of almost the same, 0.080 (Figure 2.6.8). Of the 22 GlobCover classes, a total of 16 are present in these mountains (we exclude class 230, 'no data'). Since most of the region is relatively rich in precipitation, the ground is in general covered by vegetation except for steep areas where the bedrock is exposed and where the ground is covered by large rocks draining loose material away. This is much similar to the Scandinavian Mountains; however, there are more species thriving to higher temperatures at the lower elevations than in Scandinavia.

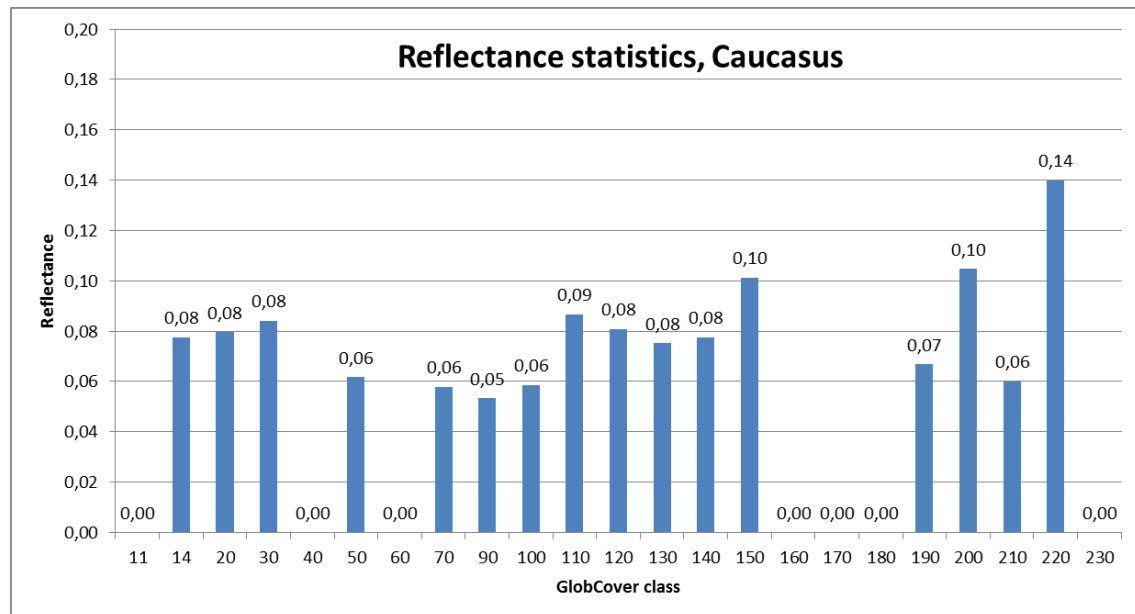


Figure 2.6.8 Reflectance statistics for the Caucasus Mountains. The numbers along the X-axis are the GlobCover class numbers.

In the Caucasus Mountains, one single class does not dominate as much as in the Scandinavian Mountains (Figure 2.6.9, left). However, classes 20 (mosaic cropland) and 30 (mosaic vegetation) dominate fairly large areas, both are mixtures of grassland, shrubland and forest. Next in dominance follows classes 50 (closed broadleaved deciduous forest) and 14 (rainfed croplands). Then follows class 150 (sparse vegetation), class 130 (closed to open shrubland) and class 110 (mosaic forest or shrubland/grassland). Most of the remaining area is composed of needle-leaved evergreen forest (class 90), mixed broadleaved and needle-leaved forest (class 100), mosaic grassland/forest or shrubland (class 120) and bare areas (class 200).

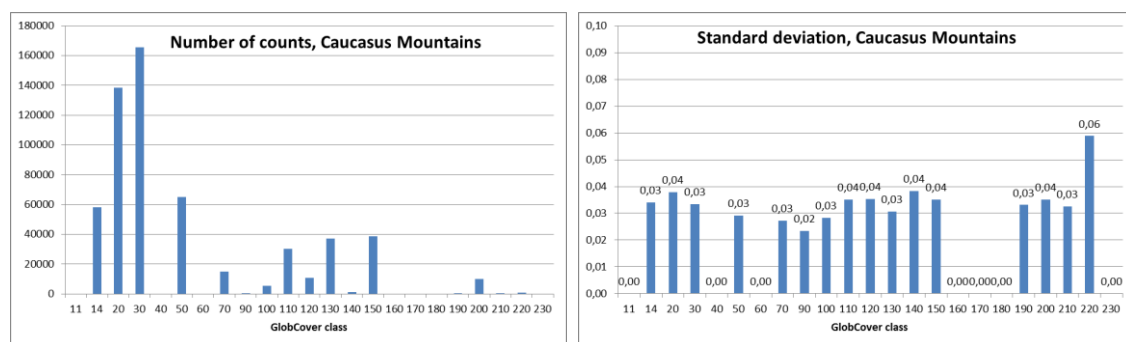


Figure 2.6.9 Left: Number of counts (observations) for the Caucasus Mountains (corresponding to the data set in Figure 2.6.8). Right: Standard deviation for the reflectance of each class.

The classes exhibit quite similar reflectance variability as the Scandinavian Mountains (Figure 2.6.9, right). The typical standard deviation is 0.03 or 0.04, which also here corresponds to almost 50% of the mean reflectance value for several classes.

Tibetan Plateau

The reflectance range of the classes is about the same for the Tibetan Plateau as for the Scandinavian Mountains, [0.03, 0.10], but with significantly lower reflectance of most classes (Figure 2.6.10). The area-weighted mean is therefore less, 0.060. Of the 22 GlobCover classes, a total of 19 are present in these mountains (we exclude class 230, 'no data'). Since most of the region is low in precipitation, the ground surface is in general significantly more arid than the Scandinavian and Caucasus Mountains. There is therefore less vegetation cover and accordingly more exposure of soil, rocks and bedrock. Less precipitation should indicate less soil moisture, and therefore higher reflectance. However, the rocks and soils (and minerals in general) seem to be of generally lower reflectance at the Tibetan Plateau than the Scandinavian and Caucasus Mountains.

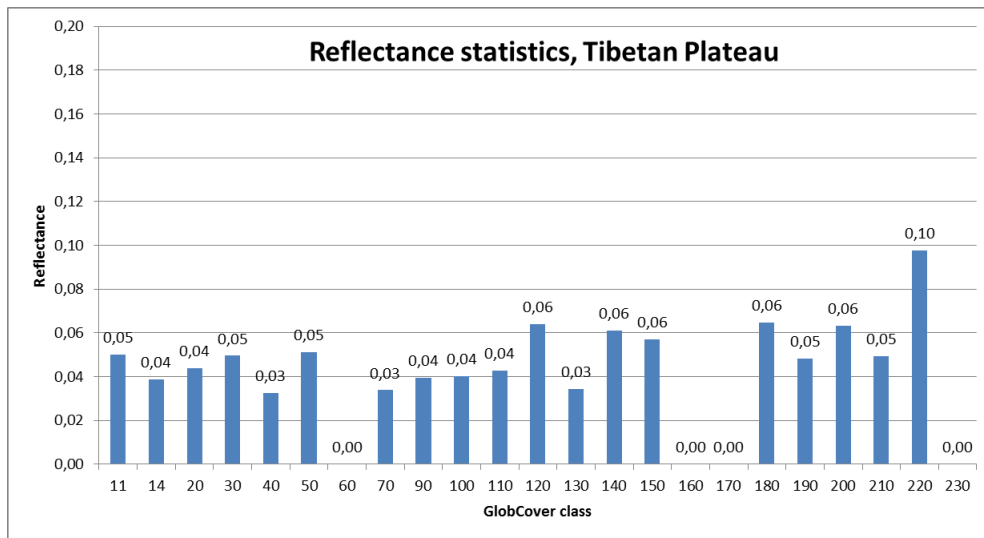


Figure 2.6.10 Reflectance statistics for the Tibetan Plateau. The numbers along the X-axis are the GlobCover class numbers.

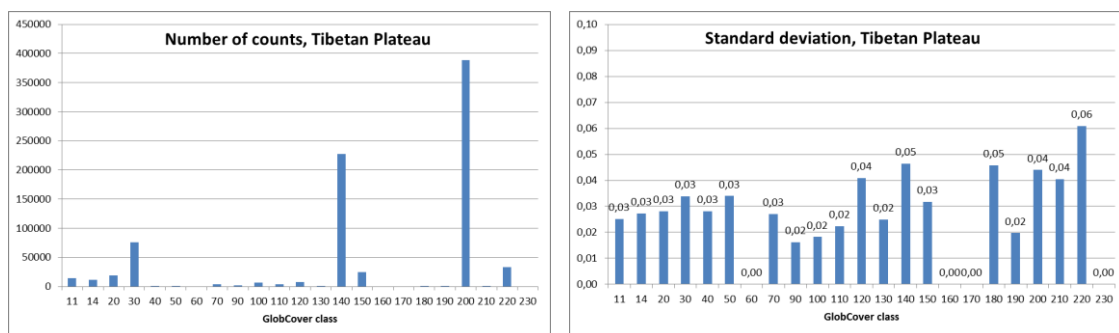


Figure 2.6.11 *Left*: Number of counts (observations) for the Tibetan Plateau (corresponding to the data set in Figure 2.6.10). *Right*: Standard deviation for the reflectance of each class.

Three classes totally dominate the reflectance of the Tibetan Plateau (Figure 2.6.11, left). Bare area (class 200) and grassland, savannahs or lichens/mosses (class 140) represent most of the surface area with some contribution from mosaic vegetation (class 30). Then there are small contributions from class 11 (post-flooding or irrigated croplands), class 14 (rainfed croplands),

class 20 (mosaic cropland), class 150 (sparse vegetation) and class 220 (permanent snow and ice). The occurrences of the remaining 11 classes are so small that they might be ignored.

The classes exhibit reflectance variability exceeding the Scandinavian and Caucasus Mountains for some classes (Figure 2.6.11, right). The typical standard deviation is in the range 0.02–0.05, more than 50% of the mean reflectance value for several classes.

Rocky Mountains

The reflectance range is smaller in the Rocky Mountains than in the other three regions, [0.02, 0.06], and has lowest reflectance of all regions for almost all classes (Figure 2.6.12). The area-weighted mean is therefore also the lowest, 0.030, much lower than for the other three regions. Of the 22 GlobCover classes, a total of 16 are present in these mountains (we exclude class 230, 'no data'). The region is variable in precipitation, many places with quite a high level of precipitation, and differs in dominating vegetation types from the other areas. Coniferous tree species dominate much of the region, and seem to be one of the principle reasons of lower reflectance. Rocks and soils also seem to be of lower reflectance than the Scandinavian and Caucasus Mountains.

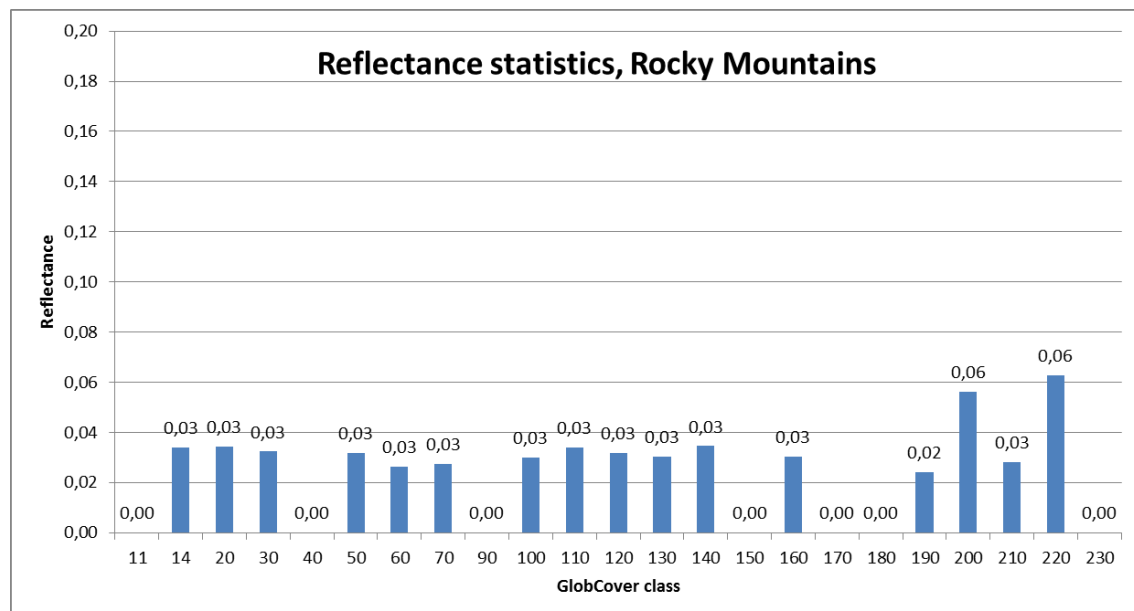


Figure 2.6.12 Reflectance statistics for the Rocky Mountains. The numbers along the X-axis are the GlobCover class numbers.

Two classes dominate the reflectance of the Rocky Mountains (Figure 2.6.13, left). Closed needle-leaved evergreen forest (class 70) and closed to open shrubland (class 130) cover most of the surface area with some contribution from mosaic vegetation (class 30) and grassland, savannas or lichens/mosses (class 140). Then there are small contributions from class 110 (mosaic forest or shrubland/grassland), class 120 (mosaic grassland/forest or shrubland), class 50 (closed broadleaved deciduous forest), class 100 (closed to open mixed broadleaved and needle-leaved forest), class 14 (rainfed croplands) and class 20 (mosaic cropland/vegetation).

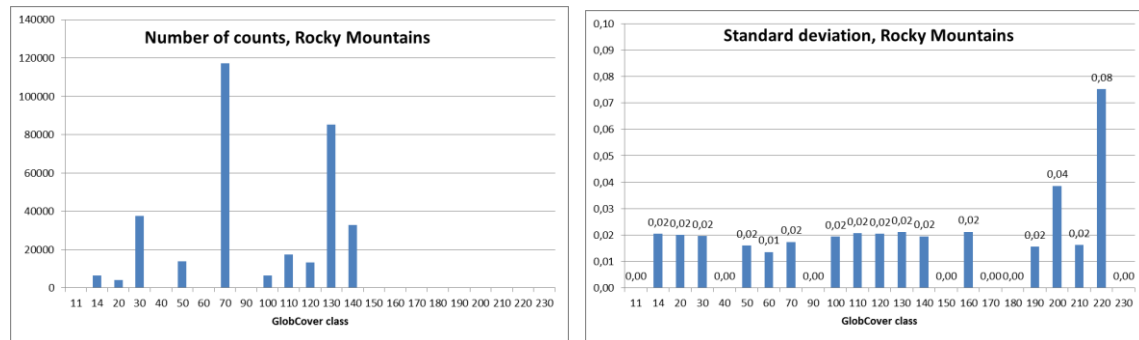


Figure 2.6.13 *Left*: Number of counts (observations) for the Rocky Mountains (corresponding to the data set in Figure 2.6.12). *Right*: Standard deviation for the reflectance of each class.

Most classes exhibit less variability than for the classes in the three former regions (Figure 2.6.13, right). The typical standard deviation is 0.02. However, this amounts to almost 50% of the mean reflectance value for most classes.

Discussion and conclusions

One should keep in mind the uncertainty associated with the results, both temporally and spatially. Moisture is known to reduce surface reflectance, in particular in the case of soil moisture. This is probably the largest source of temporal short-term variability. Furthermore, there is some reflectance uncertainty associated with the timing of snow-free ground determined and the vegetation development. Some species start greening already before all the snow is gone locally. There might also be small patches of snow left that were undetectable by the algorithm. In mountain regions cast shadows play a significant role affecting the apparent TOA reflectance. The cast-shadow pattern will change somewhat with the increasing solar elevation during the snowmelt period. This means that there might be some deviation between the snow-free ground reflectance found post-snow season and the apparent reflectance during the snowmelt period when the ground is covered with patches of snow (FSC < 100%).

Furthermore, there is significant uncertainty associated with the generalisation of reflectance values from the four regions with measurements to covering all mountains within the SE product domain. This is likely the largest source of errors with this approach.

The application of the results reported here would likely need to be balanced between the ideal accuracy locally and practical feasibility, the first calling for using local reflectance determined for each land cover class and the latter for as few classes as possible representing 'pooled' reflectance values.

The simplest approach would be to select a single 'pooled' reflectance value for mountains. The Northern Hemisphere mountain-zone area-weighted means (defined by the four zones in Figure 2.6.15) of the regional area-weighted means (the four study sites) is 0.066. Some improvement of the SE product should be obtained by using this value which, probably, is more representative for mountains than the snow-free ground reflectance value of 0.10 used previously with the SCAMod algorithm.

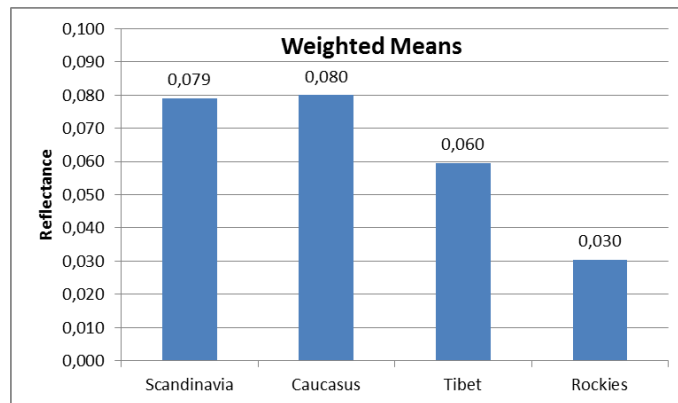


Figure 2.6.14 Area-weighted mean reflectance values for the four mountain regions studied.

The next logical alternative, in complexity, is to use a pooled area-weighted mean reflectance value for each mountain region (Figure 2.6.14). This approach would likely improve the overall accuracy of SE for mountains quite much compared to the use one pooled value as there are clear regional differences. The main challenge is, based on these four regions, to define the domains of those four values. A scenario is depicted in Figure 2.6.15 based on some, but limited, knowledge of regional reflectance variability.

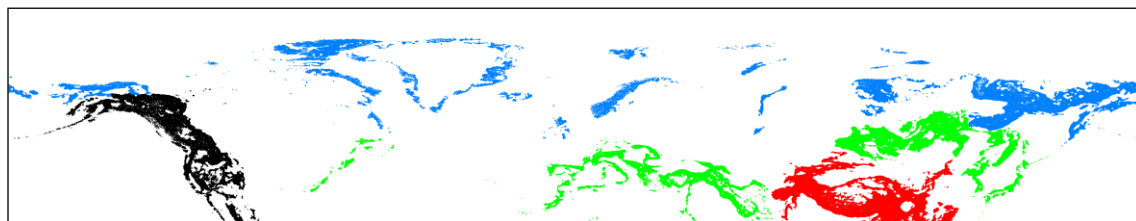


Figure 2.6.15 The scenario for distribution of the area-weighted mean reflectance values in Figure 5.1 in four zones in the Northern Hemisphere. Blue represents reflectance values from Scandinavian Mountains, green values from Caucasus Mountains, red values from Tibetan Plateau, and black values from Rocky Mountains.

As there is within-region variability between the mean reflectance values for the different land cover classes, there is further accuracy improvement to gain from using land-cover stratified reflectance values. Looking at the statistics for the Scandinavian Mountains, we see that the eight classes covering most of the region is within the reflectance range [0.07, 0.09], with the dominating class having reflectance value 0.08. Stratification into three {0.07, 0.08, 0.09} should do quite well.

For the Caucasus Mountains, the 11 classes totally dominating the region have reflectance values within the range [0.06, 0.10]. The two most dominating classes both have a reflectance value of 0.08. Number three with respect to dominance has value 0.06 and number four 0.08. The remaining 11 classes have values of 0.06, 0.08 or 0.10. Proper spectral-value stratification for the region seems to be the set {0.06, 0.08, 0.10}.

The three totally dominating classes at the Tibetan Plateau have reflectance values of (in order of dominance) 0.06, 0.06 and 0.05, respectively. The next four classes present have values 0.06, 0.04, 0.05 and 0.04. For this region proper reflectance-value stratification seems to be the set {0.04, 0.05, 0.06}.

The ten classes that represent all the area of Rocky Mountains all have reflectance value 0.03. This means that any stratification will add very little. The values of the remaining six classes that divert somewhat is 'bare areas' of value 0.06 and 'artificial surfaces and associated areas' of value 0.02. If stratifying the Rocky Mountains at all, the reflectance-value stratification would be the set {0.02, 0.03, 0.06}.

The ultimate stratification is to use all GlobCover classes with per-class reflectance values. A regional split as shown in Figure 2.6.15 could also in this case be used until, potentially, all mountains have been covered by observations of TOA reflectance using MODIS.

The four alternatives outlined above are summarised in Table 2.6.8.

Table 2.6.8 The presented alternatives for assigning specific values of snow-free ground reflectance to mountain regions in the Northern Hemisphere.

Alternative	Explanation	Scandinavian Mountains	Caucasus Mountains	Tibetan Plateau	Rocky Mountains
0	Previous solution with one global value everywhere	0.10	0.10	0.10	0.10
1	Pooled global value for the mountains	0.066	0.066	0.066	0.066
2	Region-wise mean value	0.08	0.08	0.06	0.03
3	Generalised land cover and region-wise mean values	{0.07, 0.08, 0.09} (Separate Excel sheet)	{0.06, 0.08, 0.10} (Separate Excel sheet)	{0.04, 0.05, 0.06} (Separate Excel sheet)	{0.02, 0.03, 0.06} (Separate Excel sheet)
4	Specific land cover and region-wise mean values	(Separate Excel sheet)	(Separate Excel sheet)	(Separate Excel sheet)	(Separate Excel sheet)

One should keep uncertainty in mind when choosing an alternative for the GlobSnow SE algorithm. There is the within-class variability as shown above, and there is further uncertainty when assigning the results from the four regions to all mountain regions in the Northern Hemisphere. There is probably little to gain, if anything, going from Alternative 3 to 4. The greatest improvement is probably going from Alternative 0 (using current global value), to Alternative 2, pooled regional values. As there is significant between-region variability, as the results in Chapter 4 show, Alternative 1 is not recommended. Alternative 1 should give an overall improvement compared to Alternative 0, but the region-wise deviation would still be significant.

2.6.3 Consideration of snow-free ground reflectance in the GlobSnow SE product

Since the analysis of snow-free ground reflectance was carried out for limited data set in practice, the combination of reflectance masks for plains and mountains turned out to be problematic. Since mountains and non-mountains are partly characterized by same GlobCover classes, the different snow-free ground reflectance statistics for such classes caused artificial

boundaries at the mountain borderline as identified by the mountainmask. Moreover, the analyses showed high variability for class-stratified reflectances for mountains, compared to those for plains. Variability also within each of the proposed four mountain regions was considerable, when investigated for areas not included in the actual snow-free ground reflectance analysis. Due to these reasons the production of final GlobSnow v2.0 SE exploits the reference values of snow-free ground reflectance determined from the analysis of plains.

2.7 Estimation of uncertainties

2.7.1 Introduction

Jouni Pulliainen, Miia Salminen

The uncertainty of SE product is considered by the statistical error (random error). This is different to the case of SWE product, where the total error is composed of two contributions (a) statistical random error and (b) systematic error. Statistical error is here defined as a theoretical error that can be estimated through an error propagation analysis made for the applied fractional snow cover retrieval method, eq. 2.5.2 (Metsämäki et al. 2005; Salminen et al. 2013).

Figure 2.7.1 shows the flowchart of the general process for the estimation of the product error. The uncertainty of SE product only includes the left part (systematic errors excluded as their magnitudes and behavior are unknown).

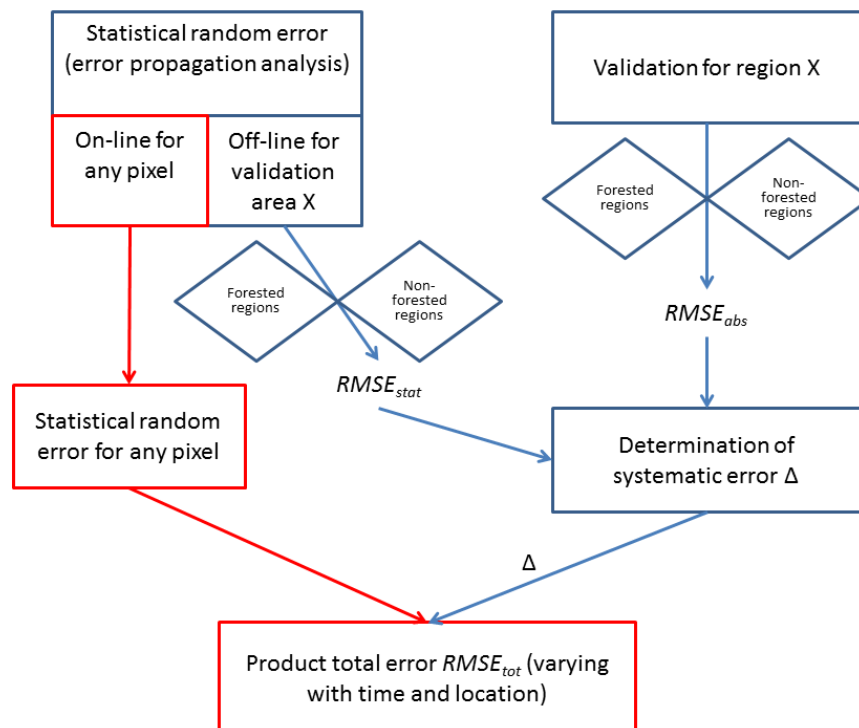


Figure 2.7.1 Procedure for the on-line determination of the product total error (SWE or fractional snow cover area, FSC). The calculation of systematic error is performed off-line with validation data set. Forested and non-forested regions can be treated separately in the determination of absolute error from the applied validation data set. In case of FSC estimation (GlobSnow v2.0 and v2.1 SE product) only the statistical error part depicted by red color is implemented, since the available reference data does not allow the detailed determination of the systematic error.

2.7.2 Uncertainties for plains

Jouni Pulliainen, Miia Salminen

The fundamental formula of the SCAMod algorithm in order to estimate the fraction of snow covered area for an individual pixel is:

$$\text{FSC} = \frac{\frac{1}{t^2} \rho_{\text{obs}} + \left(1 - \frac{1}{t^2}\right) \rho_{\text{forest}} - \rho_{\text{ground}}}{\rho_{\text{snow}} - \rho_{\text{ground}}} \quad (2.7.1)$$

The statistical accuracy of SCAMod-derived FSC can be obtained from Eq. (2.7.1) using the law of error propagation (e.g. Taylor, 1982) which gives the variance for FSC (S_{FSC}^2) as follows:

$$\begin{aligned} S_{\text{FSC}}^2(\rho_{\text{obs}}(\text{FSC}), t^2) &= \left(\frac{\partial(\text{FSC})}{\partial \rho_{\text{obs}}(\text{FSC})}\right)^2 S_{\text{obs}}^2 + \left(\frac{\partial(\text{FSC})}{\partial t^2}\right)^2 S_{t^2}^2 + \left(\frac{\partial(\text{FSC})}{\partial \rho_{\text{snow}}}\right)^2 S_{\text{snow}}^2 \\ &+ \left(\frac{\partial(\text{FSC})}{\partial \rho_{\text{forest}}}\right)^2 S_{\text{forest}}^2 \\ &+ \left(\frac{\partial(\text{FSC})}{\partial \rho_{\text{ground}}}\right)^2 S_{\text{ground}}^2 \end{aligned} \quad (2.7.2)$$

Further on, this is equal to

$$\begin{aligned} &S_{\text{FSC}}^2(\rho_{\text{obs}}(\text{FSC}), t^2) \\ &= \left(\frac{1}{t^2(\rho_{\text{snow}} - \rho_{\text{ground}})}\right)^2 S_{\text{obs}}^2 + \left(\frac{1}{(t^2)^2} \frac{\rho_{\text{forest}} - \rho_{\text{obs}}(\text{FSC})}{\rho_{\text{snow}} - \rho_{\text{ground}}}\right)^2 S_{t^2}^2 \\ &+ \left(\frac{-\frac{1}{t^2} \rho_{\text{obs}}(\text{FSC}) - \left(1 - \frac{1}{t^2}\right) \rho_{\text{forest}} - \rho_{\text{ground}}}{(\rho_{\text{snow}} - \rho_{\text{ground}})^2}\right)^2 S_{\text{snow}}^2 + \left(\frac{1 - \frac{1}{t^2}}{\rho_{\text{snow}} - \rho_{\text{ground}}}\right)^2 S_{\text{forest}}^2 \\ &+ \left(\frac{\frac{1}{t^2} \rho_{\text{obs}}(\text{FSC}) - \left(1 - \frac{1}{t^2}\right) \rho_{\text{forest}} - \rho_{\text{snow}}}{(\rho_{\text{snow}} - \rho_{\text{ground}})^2}\right)^2 S_{\text{ground}}^2 \end{aligned} \quad (2.7.3)$$

Error contribution due to observation noise

The observation noise S_{obs}^2 includes the effect of the inaccuracy of instrument, as well as the effect of other fluctuating variables not considered by other terms of (2.7.3); e.g. the influence of atmosphere to TOA reflectance. However, the effect of this term is small compared to other error contributions. Therefore, we assume $S_{\text{obs}}^2 = 0$ in the SE error calculations.

Error contribution due to two-way forest canopy transmissivity variability

As indicated by (2.7.3), the contribution due to the variance of the two-way forest canopy transmissivity (t^2) to the uncertainty of FSC retrieval is obtained by:

$$\left(\frac{\partial(\text{FSC})}{\partial t^2}\right)^2 S_{t^2}^2 = \left(\frac{1}{(t^2)^2} \frac{\rho_{\text{forest}} - \rho_{\text{obs}}(\text{FSC})}{\rho_{\text{snow}} - \rho_{\text{ground}}}\right)^2 S_{t^2}^2 \quad (2.7.4)$$

The variance of transmissivity ($S_{t^2}^2$) can be estimated from the variance of MODIS reflectances used in the transmissivity calculations for training areas. Each pixel-wise transmissivity is determined from averaged multiple reflectance observations for that pixel (see Metsämäki et al., 2012). Hence the pixel-wise variance of these reflectances is propagated into the variance of the resulting transmissivity. We calculated the typical variance of transmissivity associated to different transmissivity levels, and obtained one general formula

$$S_{t^2}^2 = (0.01 \cdot (38.8616 \cdot \exp(-19.8517 \cdot t^2) + 9.50151) \cdot t^2)^2 \quad (2.7.5)$$

Error contribution due to snow reflectance variability

Ground spectrometer derived mean and standard deviation of reflectance for wet and dry snow can be utilized in assessing their contribution to the SE estimation, see eq. (2.7.6). Based on Table 3 in Salminen et al. (2009), the applied value for S_{snow}^2 is $(0.10)^2$, and the mean value ρ_{snow} is the standard value applied in SCAMod (0.65).

$$\left(\frac{\partial(\text{FSC})}{\partial \rho_{\text{snow}}}\right)^2 S_{\text{snow}}^2 = \left(-\frac{\frac{1}{t^2}\rho_{\text{obs}}(\text{FSC}) - \left(1 - \frac{1}{t^2}\right)\rho_{\text{forest}} - \rho_{\text{ground}}}{(\rho_{\text{snow}} - \rho_{\text{ground}})^2}\right)^2 S_{\text{snow}}^2 \quad (2.7.6)$$

Error contribution due to (opaque) forest canopy reflectance variability

According to eq. 2.7.3, the error due to the contribution of forest canopy reflectance variability is

$$\left(\frac{\partial(\text{FSC})}{\partial \rho_{\text{forest}}}\right)^2 S_{\text{forest}}^2 = \left(\frac{1 - \frac{1}{t^2}}{\rho_{\text{snow}} - \rho_{\text{ground}}}\right)^2 S_{\text{forest}}^2 \quad (2.7.7)$$

The variance of (opaque) forest canopy reflectance S_{forest}^2 is currently based on relatively limited dataset and will be investigate more in future. The applied value for the variance of opaque forest canopy reflectance, S_{forest}^2 , at 555 nm is $(0.01)^2$. This value is obtained from reflectance measurements of thick layers of Scots pine branches at laboratory conditions (Niemi et al. 2012). In addition, Heinilä et al. (2013) have shown that high resolution airborne data is useful in determining the statistical behaviour of the forest canopy reflectance (mean and variance) when the canopy closure information is available. Their findings (see Figure 2.7.2) support the use of the above-mentioned value.

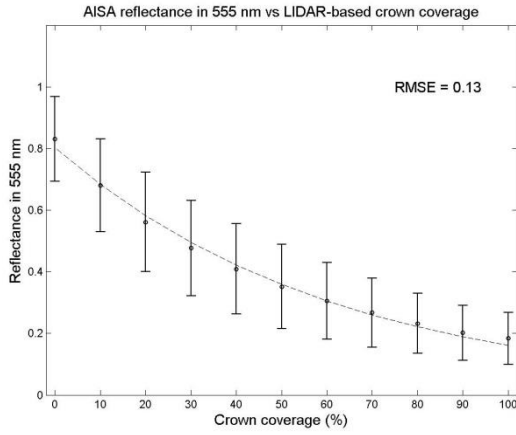


Figure 2.7.2 Green band (555 nm) mean reflectance and standard deviation is depicted for a boreal forest test site with varying Crown Coverage (CC) and snow-covered terrain. CC-values are divided into 11 classes. Mean values and standard deviations are depicted to each class. The exponential regression line between CC data and reflectance is also shown. By fitting the reflectance model to presented data, an estimate for (opaque) canopy reflectance and its variability can be obtained.

Error contribution due to snow-free ground reflectance variability

The contribution of snow-free ground reflectance to total variance is

$$\begin{aligned} & \left(\frac{\partial(\text{FSC})}{\partial \rho_{\text{ground}}} \right)^2 S_{\text{ground}}^2 \\ &= \left(\frac{\frac{1}{t^2} \rho_{\text{obs}}(\text{FSC}) + \left(1 - \frac{1}{t^2}\right) \rho_{\text{forest}} - \rho_{\text{snow}}}{(\rho_{\text{snow}} - \rho_{\text{ground}})^2} \right)^2 S_{\text{ground}}^2 \end{aligned} \quad (2.7.8)$$

where S_{ground}^2 is the variance of snow-free ground reflectance estimated for the SE product pixel under investigation. As each pixel is composed of 16 sub-grid cells that exhibit different reflectance levels depending on corresponding GlobCover class, S_{ground}^2 is given by

$$S_{\text{ground}}^2 = \sum_{c_i=1}^{N_{\text{classes}}} \left(\frac{n_i}{16} \right)^2 \text{var}(\rho_{\text{ground},c_i}) \quad (2.7.9)$$

Figure 2.7.3 shows the pixel-wise standard deviation of snow-free ground reflectance for the European test area. In addition of showing the outline of determining mean ρ_{ground} , Figure 2.6.1 shows how the variance of snow-free ground reflectance (S_{ground}^2) is determined in practice for a global application.

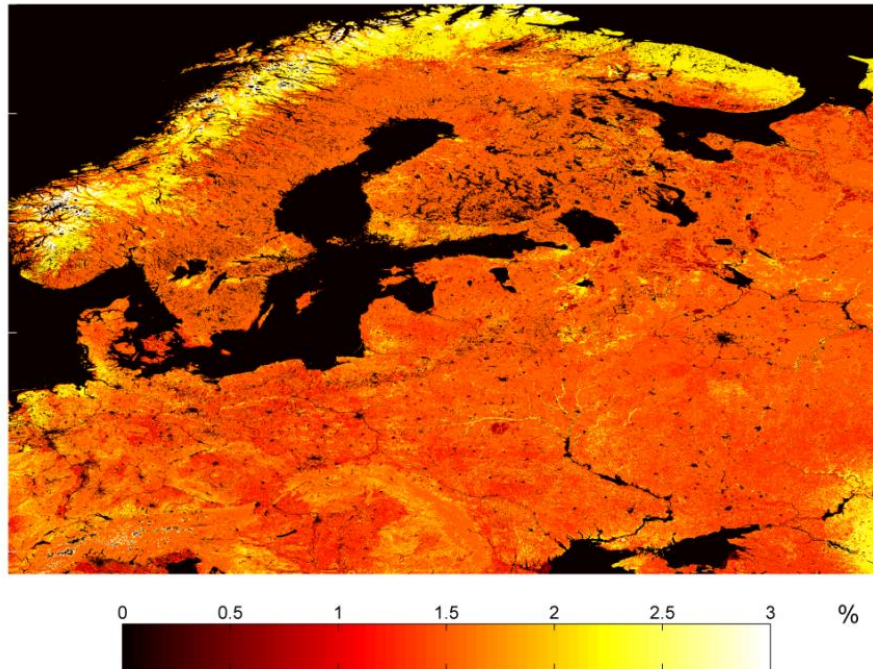


Figure 2.7.3 Retrieved map of the standard deviation of snow-free ground reflectance for the European test area (in %-units).

2.7.3 Uncertainties for mountains

Arnt-Børre Salberg and Rune Solberg

Sources that contribute to uncertainty

The method for estimating the FSC from optical satellite data is based on a high reflectance of snow compared to other natural targets. However, the estimated FSC depends on many factors, including the:

- **Transmissivity.** The factor considers the ability of the forest to transmit light from the ground to the satellite sensor. It is difficult to determine the FSC on the ground in forested areas, in particular if the forest cover is dense.
- **Terrain effects.** The terrain causes reduced illumination of some areas (“cosine” effect) and cast shadows. This applies in many spatial scales, like from large mountains to small terrain variations within a pixel.
- **Atmosphere.** Aerosols, clouds and cast shadows from clouds, not detected by the cloud detection algorithm result in noise in reflectance measurements.
- **Random component.** The random component accounts for all other factors, including model errors.

FSC uncertainty for mountains

The true FSC may be expressed as

$$FSC = \widehat{FSC} + w \quad (2.7.10)$$

where w denotes the FSC residuals. Now, assuming that w is statistical independent of \widehat{FSC} , the Mean Squared Error (MSE) of the *prediction error* is

$$MSE = E\{(FSC - \widehat{FSC})^2\} = bias(\widehat{FSC})^2 + var(\widehat{FSC}) + var(w). \quad (2.7.11)$$

If the FSC estimate is *unbiased*, the MSE reduces to the variance of the prediction error, $FSC - \widehat{FSC}$, and equals the sum of the two variance components

$$var(FSC - \widehat{FSC}) = var(\widehat{FSC}) + var(w). \quad (2.7.12)$$

The variance of \widehat{FSC} is estimated as in Section. 2.7.2, and the remaining term is estimated as

$$bias(\widehat{FSC})^2 + var(w) = MSE - var(\widehat{FSC}) \quad (2.7.13)$$

where the MSE is estimated from a geographically limited data set where we know the ground truth FSC. As in Section 2.7.2, the $bias(\widehat{FSC})^2 + var(w)$ factor is constant for all pixels, and the pixel-wise uncertainty (for pixel i) may be expressed as

$$RMSE_i = \sqrt{var(\widehat{FSC})_i + var(w) + bias(\widehat{FSC})^2}. \quad (2.7.14)$$

Terrain effects

The effects of the terrain consist of two factors: A reduction of measured reflectance due to cast shadows and residuals of the radiometric topographic correction. The case shadows may be on a sub-pixel level due to small-scale terrain variations, or include several pixels (e.g. due to cast shadows from nearby peaks).

As a model for the cast-shadow effect from the terrain in the FSC uncertainty estimation we consider the *shaded relief* or *hillshade* (Wood, 1996). The hillshade algorithm obtains the (hypothetical) illumination of a surface by determining illumination values for each pixel in the image for a given sun position. If the hillshade is estimated from a DEM with a much higher resolution than the image sensor, small-scale terrain variations may be accounted for. The output of the shaded relief algorithm is the fractional shaded area, a value between 0 and 1, where 0 corresponds to complete shadow.

To consider the effect of the terrain, we propose to down-sample (by averaging) a high-resolution (30 m) shaded relief map generated from of DEM of similar resolution (like the ASTER GDEM V2) to the sensor resolution (typically less than 250 m). By doing so, we obtain an independent terrain effect map that may be used in a similar manner as the transmissivity map. In particular, we will investigate if the FSC estimates are *biased* with respect to the proposed terrain effect map.

Figures 2.7.4 and 2.7.5 show examples of SPOT-5 images down-sampled to 25 m and 250 m, respectively, and their corresponding shaded-relief maps. From the maps we clearly see a

correspondence between the brightness values in the SPOT-5 images and the corresponding pixel values of the shaded relief maps for both 25 m and 250 m resolution.

The bias of the FSC estimator for a given true FSC value is defined as $bias = E\{\widehat{FSC}\} - FSC$, where $E\{\}$ denotes the expectation operator. When we have a 100% snow cover (FSC equals 1), the bias is negative, whereas for 0% snow cover the bias is positive. This possesses a significant challenge since the FSC is unknown (it is what we try to estimate).

We want to determine if there is a correspondence between the shaded-relief value (SR) and the bias of the estimator. To make it simple we consider a linear relationship, i.e.

$$bias(SR) = a + b \cdot SR + w, \quad (2.7.15)$$

where a and b are unknown parameters that need to be determined, and w is a statistically independent random noise component. Ideally, these parameters should be estimated for each \widehat{FSC} value, however, this may be difficult to achieve in practice.

Note that we need to construct a shaded relief image for each satellite image acquisition since the illumination geometry changes during the year.

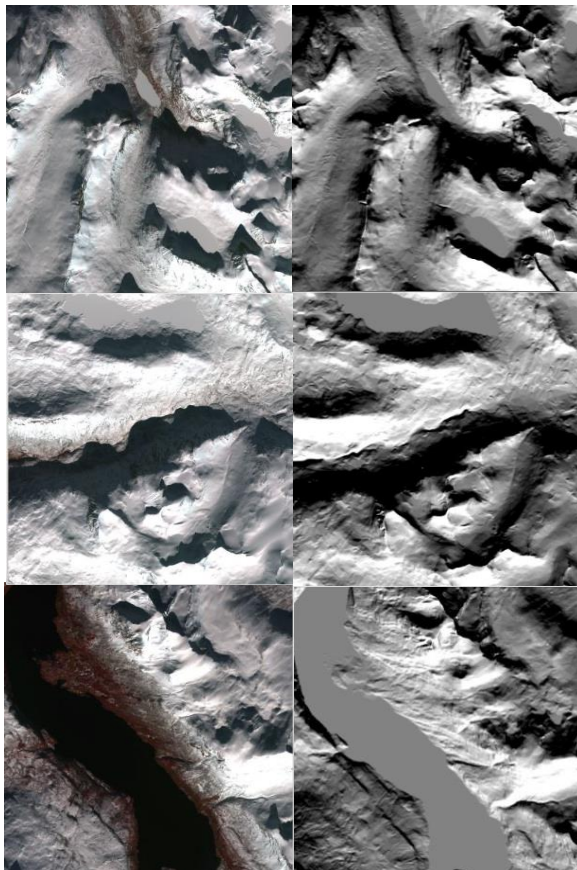


Figure 2.7.4 *Left*: SPOT 5 (band 1 to 3) down-sampled to 25 m resolution. Image acquisition of 3 April 2004 for the Narvik region in Norway (image kindly provided by the CryoLand project). *Right*: Corresponding shaded-relief maps in 25 m resolution.

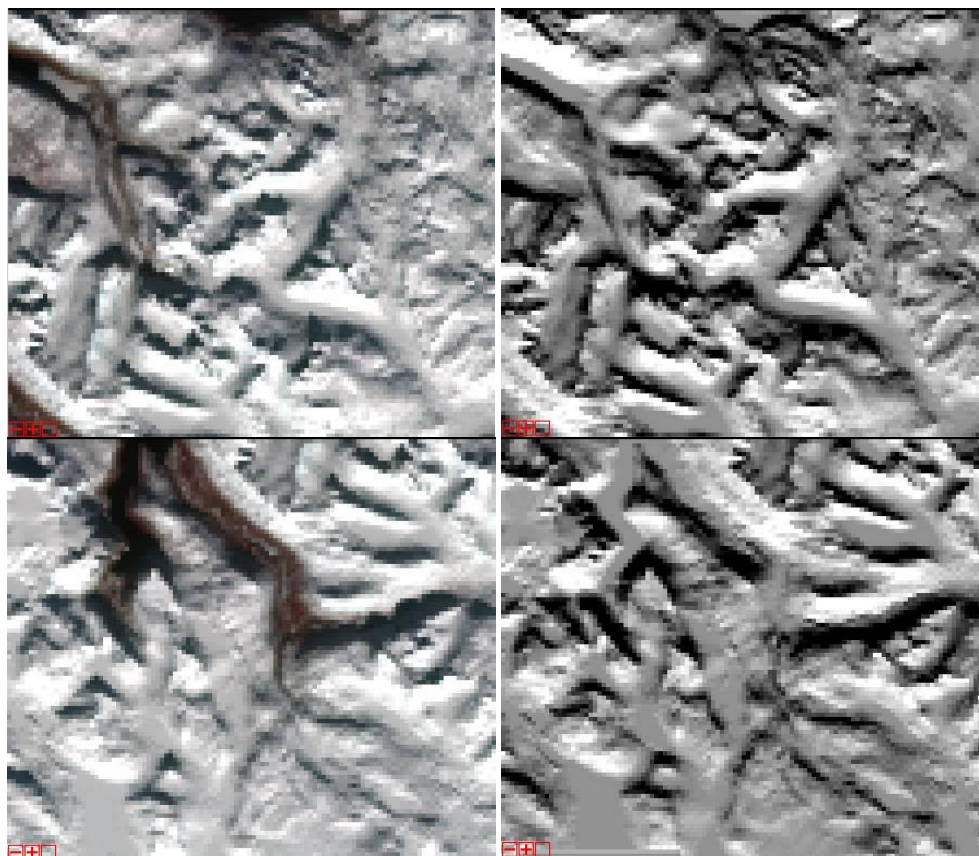


Figure 2.7.5 *Left*: SPOT 5 (band 1 -3) down-sampled to 250 m resolution. Image acquisition of 1 April 2004 for the Nord-Trøndelag region in Norway (image kindly provided by the CryoLand project). *Right*: Corresponding shaded relief maps in 250 m resolution.

Experiments and results

To evaluate the need for bias correction we consider two different regions in Norway, Narvik (April 3, 2004) and Nord-Trøndelag (April 1, 2004). For both regions the snow cover is found to be 100% by inspecting the high-resolution SPOT 5 images visually and comparing with in situ snow-depth measurements (SYNOP). All images are resampled to a geographic coordinate system with 0.01 degree resolution. For the Nord-Trøndelag image the 100% snow cover is estimated on April 1st, however, the corresponding GlobSnow SE product is from April 3rd. We do not expect any changes in snow cover between these two days.

The shaded relief maps are constructed from the 25 m national DEM for the Narvik image, and the 30 m ASTER GDEM v2 for the Nord-Trøndelag image. Both DEM's are projected in UTM33. From these elevation models a shaded relief map is calculated, down-sampled to 500 m, and finally converted into a geographical coordinate system with resolution of 0.01 degrees.

To evaluate the effect of the shaded relief, we divide the shaded-relief map into 10 intervals, [0.0, 0.1], [0.1, 0.2], ..., [0.9, 1.0], and we estimate the average bias of the corresponding interval. We then inspect the resulting plot of shaded relief versus bias. For this scatter plot we estimate the parameters a and b in the linear model using linear regression.

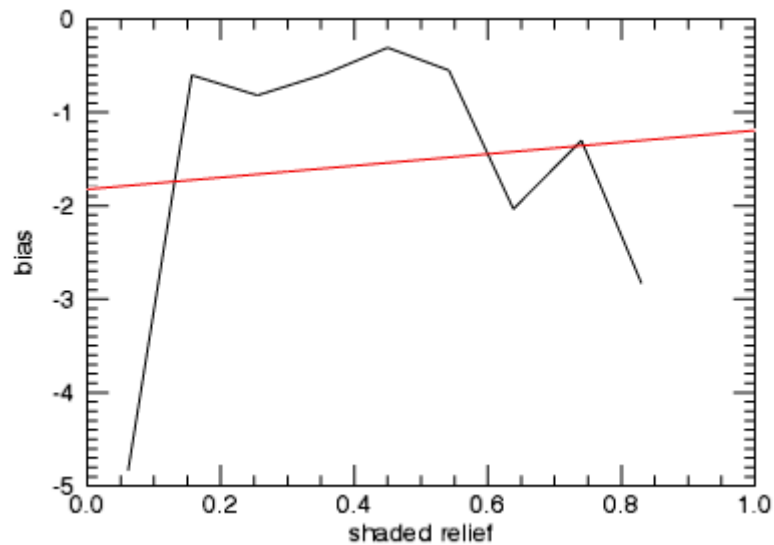


Figure 2.7.6 Shaded relief versus bias for the FSC product at Narvik, Norway, April 3rd, 2004.

For the Narvik region we observe that the bias is about -5 for shaded relief values less than 0.1 (Figure 2.7.6). For shaded relief values between 0.15 and 0.55 the bias is very small (~ -0.5), but increases for shaded-relief values larger than 0.55.

To further evaluate the distribution of bias values we estimate the probability density function (PDF) of the bias values using Parzen's estimator for three different intervals (Figure 2.7.7). The distribution for the intervals $[0.0, 0.3]$ and $[0.3, 0.6]$ confirms the observations shown in Figure 2.7.6. However, for the interval $[0.6, 1.0]$ the left tail of the estimated PDF indicates that there are some pixels with very large bias (lower panel, Figure 2.7.7).

For the Nord-Trøndelag image the bias values were smaller than -2 for all shaded relief intervals (Figure 2.7.8). The corresponding PDF plots verified this small bias (Figure 2.7.9).

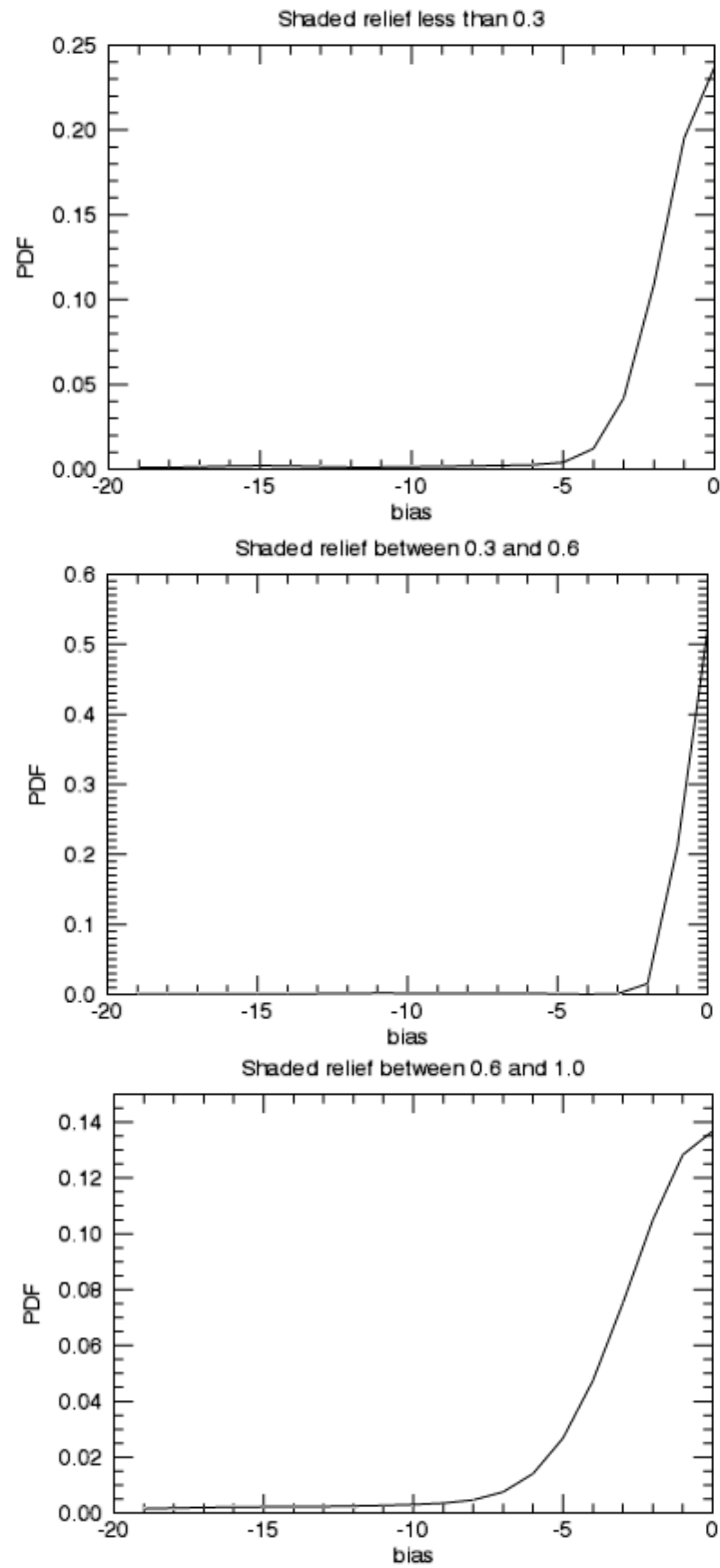


Figure 2.7.7 PDF of the bias for three different shaded relief intervals, [0.0, 0.3] (top panel), [0.3, 0.6] (middle panel), and [0.6, 1.0] (lower panel) for the Narvik region.

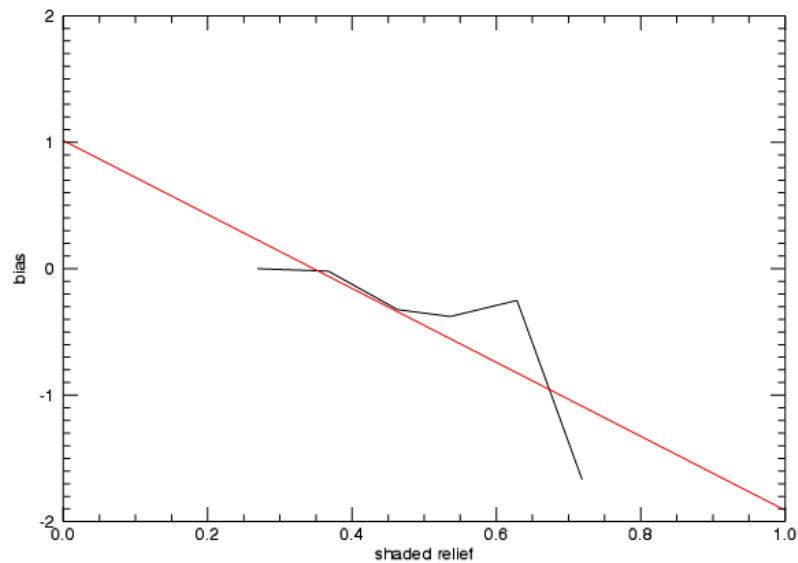


Figure 2.7.8: Shaded relief versus bias for the FSC product at Nord-Trøndelag, Norway, April 3rd, 2004.

Preliminary conclusions and recommendations

The evaluation of the bias for two regions in Norway shows that the GlobSnow Snow Extent product performs very well in mountain areas for full snow cover. The bias of the products is very small even for regions with very low shaded-relief values. Based on our very preliminary study, the need for bias correction may not be needed.

However, we have so far only investigated two sites with moderate terrain relief, and only for 100% FSC. Therefore, we cannot from the study conclude whether bias correction would be needed for conditions of FSC < 100% (patchy snow cover and snow-free). We recommend evaluating the bias for other sites and regions, including patchy and snow-free conditions. Other regions should include steeper (more alpine) terrain like the Alps, where there are severe terrain effects with large cast shadows.

Further study would require access to very-high resolution (VHR) satellite reference data where it is possible to determine the actual snow conditions and confirm the correctness visually. The radiometric quality of the data needs to be such that snow mapping in shaded areas is also possible.

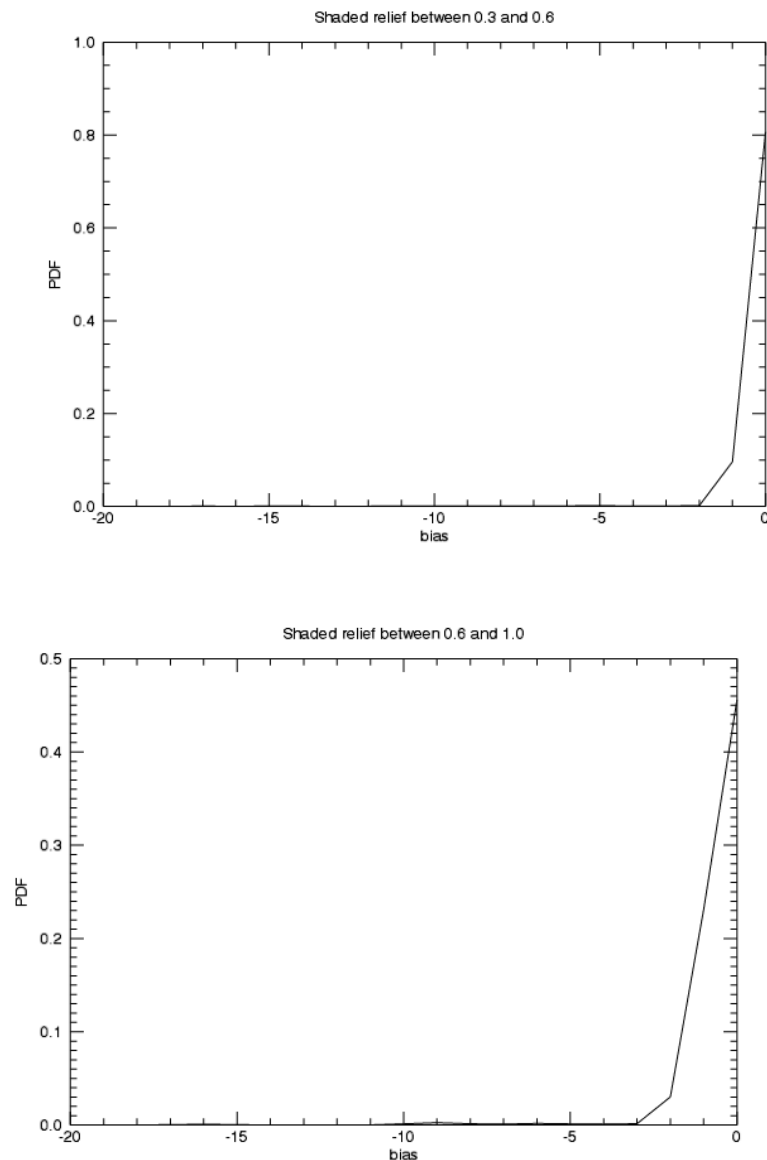


Figure 2.7.9 PDF of the bias for two different shaded relief intervals, [0.3, 0.6] (top panel) and [0.6, 1.0] (lower panel) for the Nord-Trøndelag region.

2.7.4 Combining of uncertainty models

Arnt-Børre Salberg and Rune Solberg

If further investigation of the cast-shadow effect, in particular for steeper terrain than those sites investigated in Section 2.7.4, and also for conditions of FSC < 100% lead to the conclusion that the FSC retrieval results are unbiased with respect to the terrain effect, the same uncertainty model as for plains (Section 2.7.2) can be applied. This is certainly the most attractive solution as the uncertainty estimates for the Snow Extent product will be seamless and consistent between plains and mountains. Based on this conclusion, the GlobSnow v2.0 SE product uncertainty is determined as proposed in Section 2.7.2.

However, if further analysis leads to the conclusion that bias must be taken into consideration for uncertainty estimations for mountainous regions, we suggest applying the shaded-relief approach described in Section 2.7.3. This means that a shaded-relief map needs to be constructed for each image acquisition to be used for SE product. This is feasible using ASTER GDEM V2 and the algorithm of Wood (1996) for shaded-relief map generation.

Total spatially and temporally varying error of SE product

The overall principle of the determination of SE product accuracy information is presented in Figure 2.7.1, i.e. the pixel-wise temporally and spatially varying FSC estimation error. Note, that the implementation only includes the statistical error, provided by formula (2.7.3).

2.8 Time-Series Aggregation

The Time-series aggregation block aggregates snow maps from the FSC retrieval algorithms over a given period (8 days for weekly product). FSC maps arrive the block in NRT as they are received and processed. The Time-series aggregation block stores the preliminary mosaiced FSC snow map in a temporal repository. When the aggregation period is over, the aggregation result is forwarded to the pre-processing block. The decomposition is illustrated in the diagram in Figure 2.8.1.

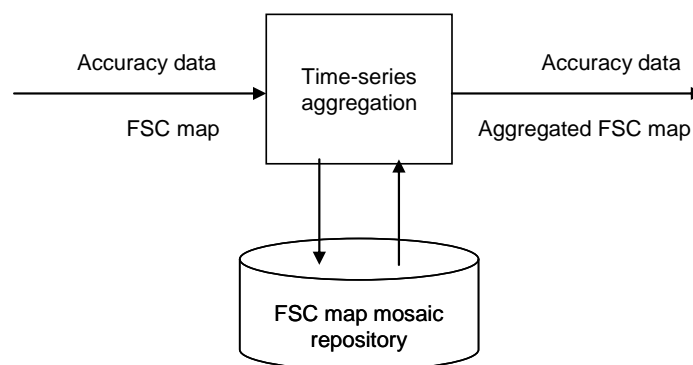


Figure 2.8.1 Decomposition of Time-series aggregation.

2.9 Post-Processing

The Product generation block generates the FSC product and the 4-class snow product, including metadata, from the input chain. The decomposition is illustrated in the diagram in Figure 2.9.1.

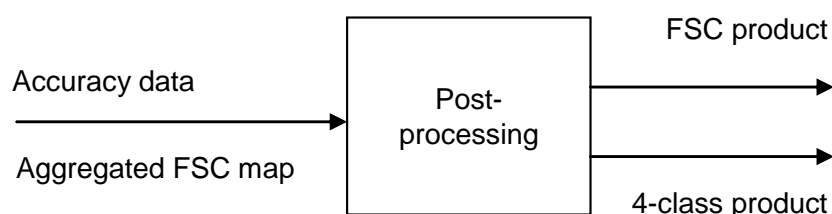


Figure 2.9.1 Decomposition of Post-processing.

In terms of FSC, the four classes represent:

- $0\% \leq \text{FSC} \leq 10\%$
- $10\% < \text{FSC} \leq 50\%$
- $50\% < \text{FSC} \leq 90\%$
- $90\% < \text{FSC} \leq 100\%$

2.10 Generation of Auxiliary Data

Gabriele Bippus, Sari Metsämäki

A set of auxiliary data is used in SE processing:

- A transmissivity map is essential to SCAMod fractional snow computation.
- A snow-free ground reflectance map used by SCAMod.

These data are used in the actual Fractional Snow Cover retrievals. The provision of these data sets is part of the conducted research work in GlobSnow-2; these are described in more detail in Sections 2.5 and 2.6.

Thematic masks are used in the GlobSnow SE processing system to 1) label areas where SE processing is not applied, such as oceans, and other open water areas and 2) to identify different kind of regions in the uncertainty calculations and 3) to derive the snow-free ground reflectance maps. The following masks are used:

- Open water mask
- Mask of mountainous areas (> 2 deg. local slope)
- Forest mask

The primary data sources for generating the masks are:

- Land cover maps from the GlobCover project with about 300 m pixel size (Bicheron et al., 2008).
- Digital elevation model (GETASSE30 DEM)

GETASSE30 stands for Global Earth Topography And Sea Surface Elevation at 30 arc second resolution. GETASSE30 is a composite of four DEM datasets. It is using the SRTM30 dataset, ACE dataset, Mean Sea Surface (MSS) data and the EGM96 ellipsoid as sources. The resulting GETASSE30 dataset represents the Earth Topography And Sea Surface Elevation with respect to the WGS84 ellipsoid at 30 arc second resolution. The GETASSE30 DEM is provided to the Brockmann Consult BEAM development team by ESA/ESRIN and is available at: <http://www.brockmann-consult.de/beam/doc/help/visat/GETASSE30ElevationModel.html>.

The data sets were processed to the resolution and projection of the SE product (latitude-longitude grid of 0.01 deg grid size).

The Open water mask was extracted from the GlobCover Regional product and includes ocean, lakes (fresh water), and rivers. First GlobCover-data were resampled to $0.025^\circ \times 0.025^\circ$ grid to gain a spatial match between 4×4 GlobCover-pixels and $0.01^\circ \times 0.01^\circ$ GlobSnow pixels. Then if number of water pixels (class 210) within the 4×4 window $\geq 4/16$, the corresponding GlobSnow pixel is labelled as Water.

Mountainous regions are identified and mapped using a smoothed slope map derived from a digital elevation model. The applied method for specifying mountainous regions is automatic and enabled the generation of a mountain mask on a global scale. The method is based on Adam et al. (2006). The mountain mask was created by applying following steps

- Calculation of the local slope from DEM (with 0.01 deg resolution).
- Masking out open water areas using water mask
- Smoothing of the local slope map using a median filter (51 x 51 pixel filter window size)
- Generation of contour line (2 deg. local slope) from the slope map
- Generation of a mask of mountain areas (local slope > 2 deg.)

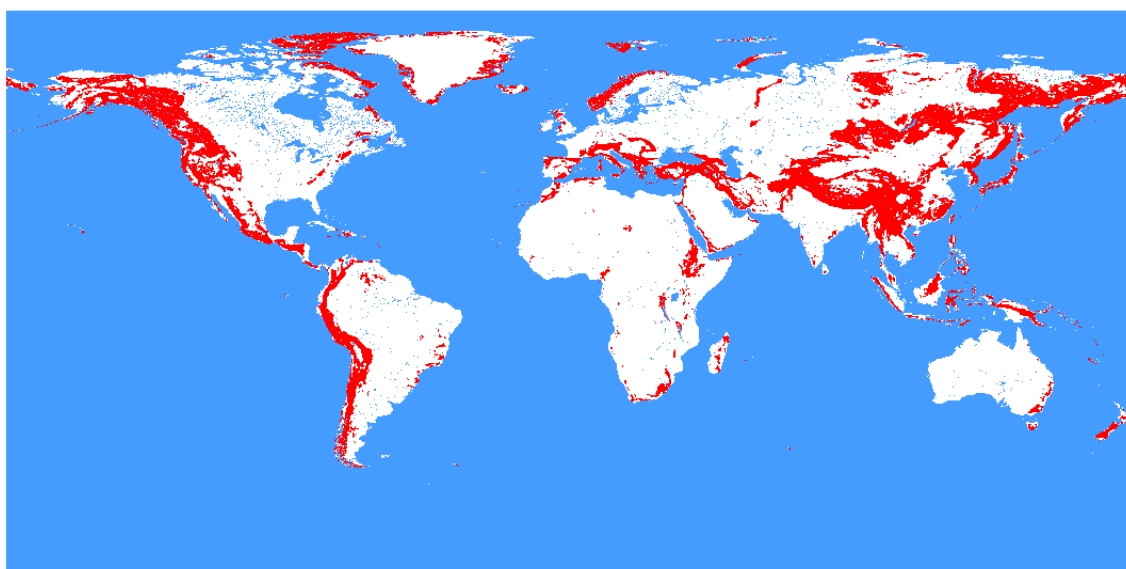


Figure 2.10.1 Combination of thematic global masks. Blue – open water, white – flat terrain; red mountainous regions with a local slope above 2 degrees.

Figure 2.10.1 shows a combination of the derived global thematic masks. Open water areas including lakes, sea and rivers appear as blue. Mountainous regions are shown in red. The main mountain ridges are located along the west coast of North- and South-America, in the Canadian Arctic, in the north-eastern part of Russia, and in south and central Europe ranging from the Iberian Peninsula over the Pyrenees, the Alps, and the Middle East to the Himalaya. Further mountain regions are located in Scandinavia, along the coast line of Greenland, in Africa, and on multiple islands all over the world.

Forest mask is used in uncertainty estimation and also in validations. The Forest mask was created based on the CORINE Land Cover 2006 (CLC2006) and GlobCover 2009 data. The CLC2006 data set, Version 16, published by the European Environment Agency (EEA) in April 2012 was used over large areas in Europe. For regions not covered by the CLC2006 product, the GlobCover 2009, Version 2.3, released by the DUE GlobCover project of ESA in December 2010 was used. The GlobCover product with $0.01^{\circ} \times 0.01^{\circ}$ pixel size was used. The CLC2006 data set with $0.0025^{\circ} \times 0.0025^{\circ}$ pixel size was resampled with the nearest neighbour method to the GlobSnow pixel size of $0.01^{\circ} \times 0.01^{\circ}$.

In the forest mask, the following codes of the Land Cover Products are included:

Corine Land Cover 2006 codes:

22 - Agro-forestry areas

23 - Broad-leaved forest

24 - Coniferous forest

25 - Mixed forest

GlobCover 2009 codes:

40 - Closed to open (>15%) broadleaved evergreen or semi-deciduous forest (>5m)

50 - Closed (>40%) broadleaved deciduous forest (>5m)

60 - Open (15-40%) broadleaved deciduous forest/woodland (>5m)

70 - Closed (>40%) needleleaved evergreen forest (>5m)

90 - Open (15-40%) needleleaved deciduous or evergreen forest (>5m)

100 - Closed to open (>15%) mixed broadleaved and needleleaved forest (>5m)

110 - Mosaic forest or shrubland (50-70%) / grassland (20-50%)

130 - Closed to open (>15%) (broadleaved or needleleaved, evergreen or deciduous) shrubland (<5m)

160 - Closed to open (>15%) broadleaved forest regularly flooded (semi-permanently or temporarily) - Fresh or brackish water

170 - Closed (>40%) broadleaved forest or shrubland permanently flooded - Saline or brackish water

Additionally to the total forest mask, the forest in mountainous areas was extracted. Therefore, the forest mask and the previously described mountain mask were combined. The resulting map includes only forest in mountains with local slopes larger than 2 degrees. Figure 2.10.2 shows the combination of the global forest mask in flat terrain and in mountainous terrain and the global water mask.

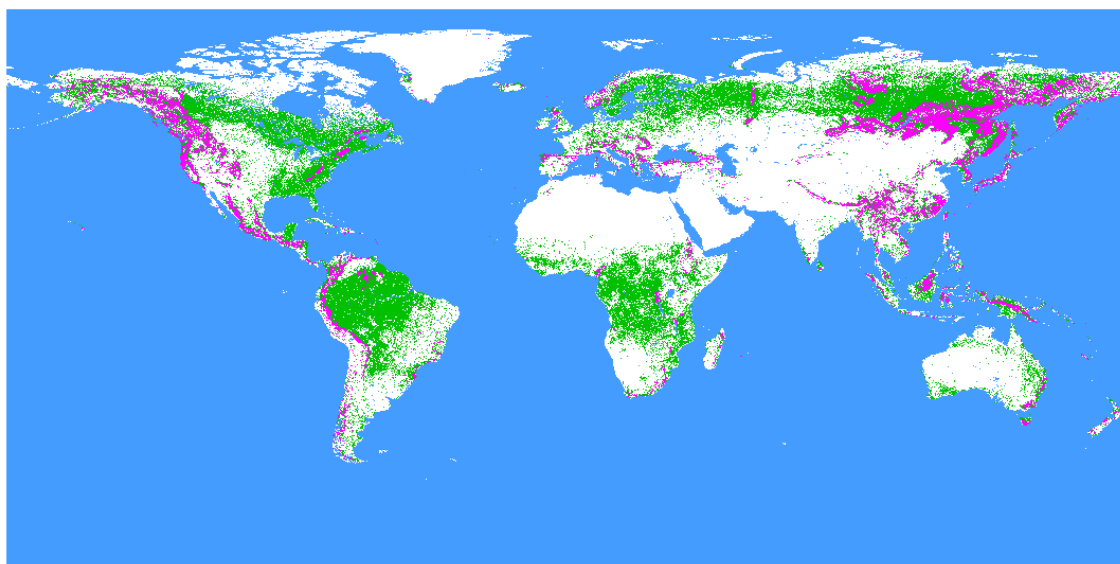


Figure 2.10.2 Combination of thematic global masks. Blue – open water, green – forest, pink – forest in mountainous regions with a local slope above 2 degrees, white – other surfaces.

3 SUMMARY

The achieved improvements targeted at i) better identification of snow in forest, related to representativeness of the Northern Hemisphere transmissivity map and ii) increasing the accuracy of FSC as to the representativeness of snow-free ground reflectance employed by SCAMod. In addition the these two, directly associated to the accuracy of FSC from GS-2 SE-product, also provision of error estimates as separate layer for each product is concerned.

Transmissivity is a key element in detection of snow under forest canopies with SCAMod method. The success of FSC-retrieval is clearly dependent on the representativeness of each pixel-wise transmissivity value. Determination of Northern hemisphere transmissivity is based on generalization of land cover class-stratified transmissivity statistics, based on MODIS reflectance data and SCAMod-method. Based on the analyses made for FSC retrievals in GlobSnow v1.2 SE products, it was concluded that the densest forests still needed a special consideration in the transmissivity map. The new transmissivity map was prepared for v2.0 SE production, exploiting GlobAlbedo. The representativeness of the new map is also shown as improved FSC-values e.g. for Russian forests at the time of full snow cover (earlier, evident underestimations were introduced). The improved capability of detecting the undercanopy snow no doubt is transmissivity value. Therefore, a strong effort was put to still better determination of transmissivities in different parts of Northern Hemisphere. The work was accomplished using basically the same approach than in GlobSnow-1, i.e. creating statistical relationship between MODIS reflectance-derived transmissivities for 'training areas' and GlobCover classification. In GlobSnow-2, however, also Global albedo (GlobAlbedo) data were employed to identify the very dense forests which are necessarily not distinguished in GlobCover. Using this approach, the densest forest were identified and accordingly, assigned with a properly low transmissivity value. The resulting transmissivity map clearly better depicts the dense boreal forests in Eurasia and in North America than the previous version applied in GlobSnow-1. The representativeness of the new map is also shown as improved FSC-values e.g. for Russian forests at the time of full snow cover (earlier, evident underestimations were introduced). The improved capability of detecting the under-canopy snow no doubt is a great advantage of GS-2 SE-product, when compared to many other methods using optical remote sensing data.

The *representativeness of snow-free ground reflectance* applied by SCAMod has great effect to the success of the FSC estimation. Using the obtained information on typical average snow-free ground reflectances for non-forested terrain types, the implications of their variations to the FSC-estimation accuracy can be assessed and quantified. We obtained statistics by extracting the representative observations (i.e. from post-melt snow-free ground) from Terra/MODIS TOA-reflectance time series for various land cover categories within Europe. The resulting land cover class-stratified reflectance statistics were used to generate snow-free ground reflectance map for the entire GlobSnow geographical domain. The results enable the determination of spatial behaviour of snow-free ground reflectance, and moreover, the investigation of the spatial behaviour of the error level resulting from the non-representative consideration of snow-free ground reflectance in the mapping of FSC. It was found that in general, the SCAMod method is applicable for FSC mapping in Europe, even if snow-free ground is treated by using a constant value for all land cover categories. However, even though the variability of the mean value of snow-free ground reflectance was relatively small in many cases, the variance from pixel to pixel was found considerable. Apart from that, there are some land cover classes, where the snow-

free ground reflectance significantly differs from the constant value of 10%-units. This was particularly revealed in analysis made for four different mountains areas in Northern Hemisphere, but also for some non-mountainous areas. For the latter, we identified those land cover classes and regions with exceptional values and refined the snow-free ground reflectance map by adding updated values. However, the pixel-wise time-series approach used so far in Europe and North America is laborious (and not feasible for obtaining global statistics as it only applies to seasonally snow-covered areas). Therefore MOD09 surface reflectance products were used to update snow-free ground reflectance statistics for the identified exceptional regions.

The calculation procedure of the *statistical error of FSC product* has been implemented and integrated with the product processing line. The consideration of total error in SE product can additionally include the contribution of systematic error. This would require the determination of total residual errors (in pixel level) from validation experiments. Further work to improve the consideration of statistical error requires, above all, the refinement of variances of different constituents of SCAMod which are the uncertainties (error variances) of two-way forest canopy transmissivity, wet snow reflectance, snow-free ground reflectance and forest canopy reflectance (opaque canopy). As these parameters are typically determined from satellite observations (TOA reflectances), they include contributions due to variations in illumination and atmospheric conditions.

The main effects creating *uncertainty specific for mountains* are: A reduction of measured reflectance due to cast shadows and residuals of the radiometric topographic correction. The cast shadows may be on a sub-pixel level due to small-scale terrain variations, or include several pixels. To determine whether there is a bias associated with the methodology used to estimate uncertainty in the plains for mountains, we studied two cases of mountain regions in Norway where we had access to SPOT-5 images, representing high enough spatial resolution to determine the actual snow cover (which turned out to be 100% in both cases). The results show that the SCAMod algorithm gives unbiased FSC retrieval in those cases. This indicates that the approach for uncertainty estimation used for plains might work for mountains as well. However, we do not know how it will work with stronger terrain relief (e.g. the Alps) or for patchy snow conditions. To make a sound conclusion possible, very-high resolution data to determine the true FSC would be needed for cases of patchy snow cover and stronger terrain relief. Meanwhile, we rely on the assumption that it is assumed that the FSC retrieval results are unbiased with respect to the terrain effect and independent of the true fractional snow cover, and applied the same uncertainty model as for plains for the entire GlobSnow geographical domain. This is certainly the most attractive solution as the uncertainty estimates for the Snow Extent product will be seamless and consistent between plains and mountains.

4 REFERENCES

- AATSR Handbook, ESA, available at <http://envisat.esa.int/handbooks/aatsr/> , last time accessed on 2009/08/18.
- Adam, J.C., Clark, E.A., Lettenmaier, D.P. and Wood, E.F. (2006). Correction of Global Precipitation Products for Orographic Effects. *J. Climate*, 19, 15–38.
- Anderson G.P., Kneizys, F. X., Chetwynd, J. H., Wang, J., Hoke, M. L., Rothman, L.S., Kimball, L.M. & McClatchey, R.A. (1995). FASCODE/MODTRAN/LOWTRAN Past/Present/Future, *Proceedings of the 18th annual Review Conference on Atmospheric Transmission Models*, 06–08 June 1995.
- Barlage, M., Zeng, X., Wei, H. and Mitchell, K. (2005). A global 0.05° maximum albedo dataset of snow-covered land based on MODIS observations. *Geophysical Research Letters* 32(17): doi: 10.1029/2005GL022881. issn: 0094-8276.
- Berk, A., Bernstein, L. S., and Robertson, D. C. (1989). MODTRAN: a moderate resolution model for LOWTRAN7, GLTR-89- 0122, Air Force Geophys. Lab., Hanscom AFB, MA, 38pp
- Berthelot, B. (2003). Coefficients SMAC pour MSG. Tech. rep., Noveltis Internal Report NOV-3066-NT-834.
- Betts, A. K., and Ball, J. H. (1997). Albedo over the boreal forest. *Journal of Geophysical Research*, 102(D24), 28,901–28,909, doi:10.1029/96JD03876.
- Bicheron, P., Huc, M., Henry, C. and Bontemps, S. (2008). *GLOBCOVER Products Description Manual*. ESA Project GLOBCOVER, GLOBCOVER_PDM_I2.2, Issue 2, Revision 2.
- Bontemps, S., Defourny, P. & Van Bogaer, E., 2010. *GLOBCOVER 2009 Products Description and Validation Report*. ESA Project GLOBCOVER.
- Heinilä, K., Salminen, M., Pulliainen, J., Cohen, J., Metsämäki, S., and Pellikka, P. (2014). The effect of boreal forest canopy to reflectance of snow covered terrain based on airborne imaging spectrometer observations. *International Journal of Applied Earth Observation and Geoinformation*, 27, 31-41.
- Manninen, T. and Stenberg, P. (2009). Simulation of the effect of snow covered forest floor on the total forest albedo, *Agricultural and forest meteorology* 149, 303-319.
- Metsämäki, S., Anttila, S., Huttunen, M. and Vepsäläinen, J. (2005). A feasible method for fractional snow cover mapping in boreal zone based on a reflectance model. *Remote Sensing of Environment*, 95, 77-95.
- Metsämäki, S., Mattila, O.-P., Pulliainen, J., Niemi, K., Luojus, K. and Böttcher, K. (2012). An optical reflectance model-based method for fractional snow cover mapping applicable to continental scale. *Remote Sensing of Environment*, 123, 508-521.

- Meyer, P., Itten, K. I., Kellenberger, T., Sandmeier, S. and Sandmeier, R. (1993). Radiometric corrections of topographically induced effects on Landsat TM data in an alpine environment. *ISPRS Journal of Photogrammetry and Remote Sensing*, 48, 17–28.
- Moody, E. G., King, M. D., Schaaf, C. B. and Hall, D. K. (2007). Northern Hemisphere fiveyear average (2000–2004) spectral albedos of surfaces in the presence of snow: Statistics computed from Terra MODIS land products. *Remote Sensing of Environment*, 111, 337–345.
- Müller, J.-P., et al. (2012). The ESA GlobAlbedo Project for mapping the Earth's land surface albedo for 15 Years from European Sensors., paper presented at IEEE Geoscience and Remote Sensing Symposium (IGARSS) 2012, IEEE, Munich, Germany, 22–27.07.2012.
- Niemi, K., Metsämäki, S., Pulliainen, J., Suokanerva, H., Böttcher, K., Leppäranta, M. and Pellikka, P. (2012). The behaviour of mast-borne spectra in a snow-covered boreal forest. *Remote Sensing of Environment*, 124, 551-563.
- Pulliainen, J. (2006), Mapping of snow water equivalent and snow depth in boreal and sub-arctic zones by assimilating space-borne microwave radiometer data and ground-based observations. *Remote Sensing of Environment*, 101:257-269.
- Rahman, H. and Dedieu, G. 1994: SMAC: A simplified method of atmospheric correction of satellitemeasurements in the solar spectrum. *International Journal of Remote Sensing*, 15, 123-143.
- Riazanoff, S., 2005. Envisat MERIS Geometry Handbook, VT-P194-DOC-001-E, V1.5. <http://www-igm.univ-mlv.fr/~riazano/publications/VT-P194-DOC-001-E-01-05.pdf>
- Salminen, M., Pulliainen, J., Metsämäki, S., Kontu, A. and Suokanerva, H. (2009). The behaviour of snow and snow-free surface reflectance in boreal forests: Implications to the performance of snow covered area monitoring. *Remote Sensing of Environment*, 113, 907-918.
- Salminen, M., Pulliainen, J., Metsämäki, S., Böttcher, K. and Heinilä, K. (2013). MODIS-derived snow-free ground reflectance statistics of selected Eurasian non-forested land cover types for the application of estimating fractional snow cover. *Remote Sensing of Environment*, 138, 51-64.
- Stow, D. A., Hope, A, McGuire, D., Verbyla, D., Gamon, J., Huemrich, F., Houston, S., Racine, C., Sturm, M., Tape K., Hinzman, L., Yoshikawa, K., Tweedie, C., Noyle, B., Silapaswan, C., Douglas, D., Griffith, B., Jia, G., Epstein, H., Walker, D., Daeschner, S., Petersen, A., Zhou, L., & Myneni, R. (2004). Remote sensing of vegetation and land-cover change in Arctic tundra ecosystems. *Remote Sensing of Environment*, 89, 281-308.
- Takala, M., Luojus, K., Pulliainen, J., Derksen, C., Lemmetyinen, J., Kärnä, J. -P., Koskinen, J. and Bojkov, B. (2011). Estimating northern hemisphere snow water equivalent for climate research through assimilation of space-borne radiometer data and groundbased measurements. *Remote Sensing of Environment*, 115, 3517–3529.
- Taylor, J. R. (1982). An introduction to error analysis. The study of uncertainties in physical measurements. (pp. 270). Oxford University Press.

Teillet, P. M., Guindon, B & Goodenough, D. G. (1982). On the slope-aspect correction of multispectral scanner data. *Canadian Journal of Remote Sensing*, 8, 84–106.

Wood, J. (1996). *The Geomorphological Characterization of Digital Elevation Models*. Ph. D. Thesis, University of Leicester, Department of Geography, Leicester, UK.